

Tensorial Neural Networks: Generalization of Neural Networks and Application to Model Compression

Jiahao Su¹, Jingling Li², Bobby Bhattacharjee², Furong Huang²

¹Department of Electrical and Computer Engineering, University of Maryland, College Park

²Department of Computer Science, University of Maryland, College Park

jiahaosu@terpmail.umd.edu, {jingling, bobby, furongh}@cs.umd.edu

Abstract

We propose *tensorial neural networks (TNNs)*, a generalization of existing neural networks by extending tensor operations on low order operands to those on high order ones. The problem of parameter learning is challenging, as it corresponds to hierarchical nonlinear tensor decomposition. We propose to solve the learning problem using stochastic gradient descent by deriving nontrivial back-propagation rules in generalized tensor algebra we introduce. Our proposed TNNs has three advantages over existing neural networks: (1) TNNs naturally apply to high order input object and thus preserve the multi-dimensional structure in the input, as there is no need to flatten the data. (2) TNNs interpret designs of existing neural network architectures. (3) Mapping a neural network to TNNs with the same expressive power results in a TNN of fewer parameters. TNN based compression of neural network improves existing low-rank approximation based compression methods as TNNs exploit two other types of *invariant structures*, periodicity and modulation, in addition to the low rankness. Experiments on LeNet-5 (MNIST), ResNet-32 (CIFAR10) and ResNet-50 (ImageNet) demonstrate that our TNN based compression outperforms (5% test accuracy improvement universally on CIFAR10) the state-of-the-art low-rank approximation based compression methods under the same compression rate, besides achieving orders of magnitude faster convergence rates due to the efficiency of TNNs.

1 Introduction

Modern neural networks [13, 16, 22, 31, 33, 34] achieve unprecedented accuracy over many difficult learning problems at the cost of deeper and wider architectures with overwhelming number of model parameters. The large number of model parameters causes repeated high-cost in predictions, which becomes a practical bottleneck when these neural networks are deployed on constrained devices, such as smartphones and Internet of Things (IoT) devices.

One fundamental problem in deep learning research is to design neural network models with compact architectures, but still maintain comparable expressive power as large models. To achieve this goal, two complementary approaches are adopted in the community: one approach is to compress well-trained neural networks while preserving their predictive performance as much as possible [3]. Another approach is to find better architectures for neural network designs such as grouping the filters into inception modules [33, 34] or bottleneck layers [14, 25].

To address this aforementioned fundamental problem, we propose *tensorial neural networks (TNNs)*, which allows not only compression of well-trained networks, but also exploration of better designs in network architectures. TNN is a generalization of existing neural networks (NNs) where matrix-vector multiplication (in fully connected layer and recurrent layers) and convolution (in convolutional layer) are extended to *generalized tensor operations*. To achieve this, we introduce new tensor algebra to extend existing operations with low order operands to those with high order operands (see Section 2 and Appendix C for details).

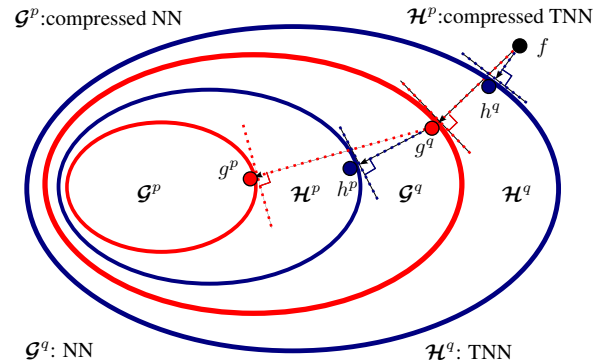


Figure 1: Relationship between NNs and TNNs. In the figure, f is the target concept. (1) **Learning** of a NN with q parameters results in g^q that is closest to f in \mathcal{G}^q , while learning of a TNN with q number of parameters results in h^q that is closest to f in \mathcal{H}^q . Apparently, h^q is closer to f than g^q . (2) **Compression** of a pre-trained NN g^q to NNs with p parameters ($p \leq q$) results in g^p that is closest to g^q in \mathcal{G}^p , while compressing of g^q to TNNs with p parameters results in h^p that is closest to g^q in \mathcal{H}^p . Apparently, the compressed TNN h^p is closer to the pre-trained g^q than the compressed NN g^p .

Figure 1 illustrates the relationship between existing neural networks and our proposed tensorial neural networks. Let \mathcal{G}^q and \mathcal{H}^q denote the sets of functions that can be represented by existing NNs and our TNNs, both with at most q parameters. Since existing NNs are special cases of TNNs, we have the following properties: (1) for any $q > 0$, $\mathcal{G}^q \subseteq \mathcal{H}^q$ and (2) there exists $p \leq q$ such that $\mathcal{H}^p \subseteq \mathcal{G}^q$. The first property indicates that TNNs are generalization of NNs while the second property guarantees that TNNs can be used for compression of NNs.

The input to a TNN is a tensor of any order m , and the TNN reduces to a normal NN if the input is a vector ($m = 1$) or a matrix ($m = 2$). **Prediction** in TNNs is similar to traditional NNs: the input is passed through the layers of a TNN in a feedforward manner, where each layer is a generalized tensor (multilinear) operation between the *high-order* input and the *high-order* weight kernels followed by a nonlinear activation function such as ReLU. **Learning** parameters in a TNN is equivalent to hierarchical nonlinear tensor decomposition, which is hard for arbitrary TNN architectures. We introduce a suite of generalized tensor algebra, which allows easy derivation of backpropagation rules and a class of TNN architectures (detailed in Appendices D, G and H). With these backpropagation rules, TNNs can be efficiently learned by standard *stochastic gradient descent*.

TNNs can be used for compression of traditional neural networks, since our proposed TNNs naturally identify *invariant structures* in neural networks (justified in section 4). Given a pre-trained NN $g^q \in \mathcal{G}^q$, compressing it to a TNN with p parameters results in h^p that is closest to g^q in \mathcal{H}^p as depicted in Figure 1. It proceeds in two steps: (1) **data tensorization**: the input is reshaped into an m -order tensor; and (2) **knowledge distillation**: mapping from a NN to a TNN using layer-wise data reconstruction.

We demonstrate the effectiveness of compression using tensorial neural networks by conducting a set of experiments on several benchmark computer vision datasets. We compress ResNet-32 on the CIFAR10 dataset by 10x with a degrading of only 1.92% (achieving an accuracy of 91.28%). Experiments on LeNet-5 (MNIST), ResNet-32 (CIFAR10) and ResNet-50 (ImageNet) demonstrate that our TNN compression outperforms (5% test accuracy improvement universally on CIFAR10) the state-of-the-art low-rank approximation techniques under same compression rate, besides achieving orders of magnitude faster convergence rates due to the efficiency of TNNs.

Contributions of this paper

1. We propose a new framework of tensorial neural networks that extends traditional neural networks, which naturally preserve multi-dimensional structures of the input data (such as videos).
2. We introduce a system of *generalized tensor algebra* for efficient learning and prediction in TNNs. In particular, we are the first to derive and analyze backpropagation rules for generalized tensor operations.
3. We apply tensorial neural networks to effectively compress existing neural networks by exploiting additional invariant structures in both data and parameter spaces,

therefore reduce the complexity of the model (the number of parameters).

4. We provide interpretations of famous neural network architectures in computer vision using our proposed TNNs. Understanding of why some existing neural network architectures are successful in practice could lead to more insightful neural network designs.

1.1 Related Works

Relation to Tensor Networks. Tensor networks are widely used in quantum physics [27], numerical analysis [11] and recently machine learning [5, 6]. Different from existing tensor networks, (1) our TNNs have nonlinearity on the edges between the tensors; and (2) TNNs are constructed as deep compositions of interleaving *generalized tensor operations* and nonlinear transformations, similar to feedforward neural networks. Furthermore, while tensor networks are still multi-linear and thus can be learned by algorithms such as power iteration [35] or alternative least squares [7], TNNs require decomposition of nonlinear (no longer multi-linear) hierarchical tensor networks.

Compression of Neural Networks. A recent survey [3] reviews state-of-the-art techniques for compressing neural networks. These techniques can be grouped into two categories: (1) compressing an existing model and (2) novel compact designs. The first category includes *low-rank approximations* [9, 18, 19, 23], *knowledge distillation* [1, 10, 15, 30] and *quantization* [8, 12, 17, 29, 38]; while the second category includes *compact designs of filters* [2, 32, 37] and *compact designs of architectures* [4, 13, 16, 33, 34]. When our TNNs are used for compression, we project an existing neural network to the class of TNNs with fewer parameters, and in Section 5, we demonstrate this projection naturally corresponds novel compact architecture.

2 Generalized Tensor Algebra

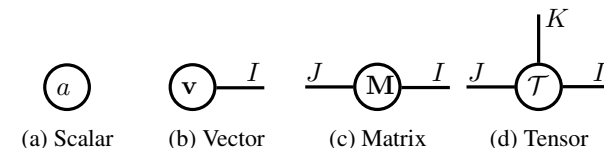


Figure 2: **Tensor Diagrams** of a scalar $a \in \mathbb{R}$, a vector $\mathbf{v} \in \mathbb{R}^I$, a matrix $\mathbf{M} \in \mathbb{R}^{I \times J}$, and a 3-order tensor $\mathcal{T} \in \mathbb{R}^{I \times J \times K}$.

Notations. An m -dimensional array \mathcal{T} is defined as an m -order tensor $\mathcal{T} \in \mathbb{R}^{I_0 \times \dots \times I_{m-1}}$. Its $(i_0, \dots, i_{n-1}, i_{n+1}, \dots, i_{m-1})^{\text{th}}$ *mode- n fiber*, a vector along the n^{th} axis, is denoted as $\mathcal{T}_{i_0, \dots, i_{n-1}, i_{n+1}, \dots, i_{m-1}}$.

Tensor Diagrams. Following the convention in quantum physics [11, 27], Figure 2 introduces *tensor diagrams*, graphical representations for multi-dimensional objects. In tensor diagrams, an array (scalar/vector/matrix/tensor) is represented as a *node* in the graph, and its *order* is denoted by the number of *edges* extending from the node, where each edge corresponds to one *mode* (whose *dimension* is denoted by the number associated to the edge).

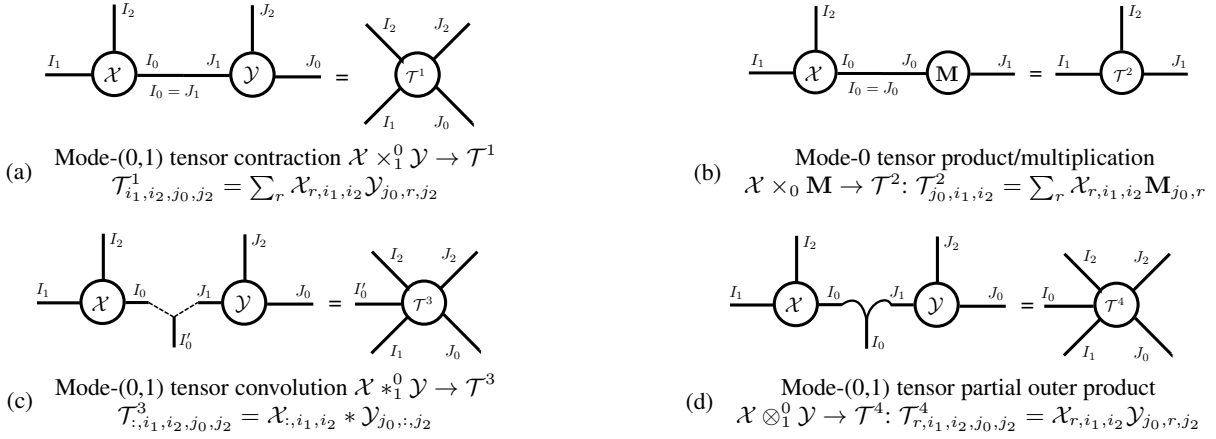


Figure 3: **Generalized tensor operations.** Examples of tensor operations in which $\mathbf{M} \in \mathbb{R}^{J_0 \times J_1}$, $\mathcal{X} \in \mathbb{R}^{I_0 \times I_1 \times I_2}$ and $\mathcal{Y} \in \mathbb{R}^{J_0 \times J_1 \times J_2}$ are input matrix/tensors, and $\mathcal{T}^1 \in \mathbb{R}^{I_1 \times I_2 \times J_0 \times J_2}$, $\mathcal{T}^2 \in \mathbb{R}^{J_0 \times I_1 \times I_2}$, $\mathcal{T}^3 \in \mathbb{R}^{I'_0 \times I_1 \times I_2 \times J_0 \times J_2}$ and $\mathcal{T}^4 \in \mathbb{R}^{I_0 \times I_1 \times I_2 \times J_0 \times J_2}$ are output tensors of corresponding operations. Similar definitions apply to general mode- (i, j) tensor operations. Existing tensor operations are only defined on lower-order \mathcal{X} and \mathcal{Y} such as matrices and vectors.

Generalized Tensor Operations. We introduce *generalized tensor operations* on *high-order tensor operands* that consist of four primitive operations in Figure 3, extending the usual operations with vector or matrix operands. In tensor diagrams, an operation is represented by linking edges from the input tensors, where the type of operation is denoted by the shape of line that connects the nodes: solid line stands for *tensor contraction* or *tensor multiplication*, dashed line represents *tensor convolution*, and curved line is for *tensor partial outer product*. We illustrate our generalized tensor operations via simple examples where third-order operands \mathcal{X} and \mathcal{Y} are considered in Figure 3. However, our generalized tensor operations can extend to higher-order tensors as rigorously defined in Appendix C.

3 Tensorial Neural Networks

A traditional convolutional neural network using tensor diagram is depicted in Figure 4a. We propose a richer class of functions, tensorial neural networks (TNNs), whose the input are tensors of any order (denoted m) and operations are generalized tensor operations. TNN are generalization of traditional neural networks: if the input is a vector and operation is matrix-vector multiplication, TNN reduces to *multi-layer perceptrons (MLP)*; and if the input is a feature map and operation is convolution, TNN reduces to *convolutional neural networks (CNN)*. The order of the input tensor and the type of the generalized tensor operation are hyperparameters that define the *architecture* of a TNN. In this paper, we design a number of successful architectures of tensorial neural networks (see Appendices G and H), and an example of *Tensor-train TNN* is illustrated in Figure 4b.

3.1 One-layer of TNN vs One-layer of CNN

In CNN, each linear layer is a special convolution operation between a *low-order* input and another *low-order* weights kernel. In contrast, each layer in TNN is characterized by a generalized tensor operation between a *high-order* input and

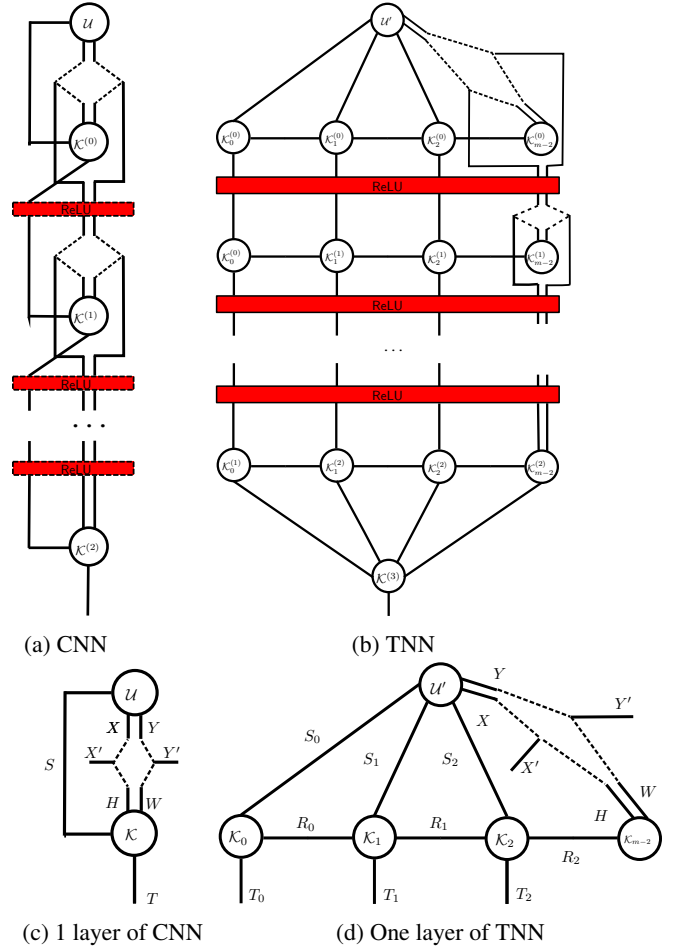


Figure 4: **Tensor diagram** of CNNs and TNNs.

another *high-order* weights kernel, allowing for higher expressive power.

One-layer of CNN A convolutional layer in traditional neural networks is parameterized by a 4-order kernel $\mathcal{K} \in \mathbb{R}^{H \times W \times S \times T}$, where H, W are height/width of the filters, and S, T are the numbers of input/output channels. The layer maps a 3-order input tensor $\mathcal{U} \in \mathbb{R}^{X \times Y \times S}$ to another 3-order output tensor $\mathcal{V} \in \mathbb{R}^{X' \times Y' \times T}$, where X, Y and X', Y' are heights/widths of the input and output feature maps.

$$\mathcal{V} = \mathcal{U} (*_0^0 \circ *_1^1 \circ \times_2^2) \mathcal{K} \quad (1)$$

We define such an operation as *compound operation*, where multiple edges are linked simultaneously (see Figure 4c for the tensor diagram of a convolutional layer). General compound operations are discussed systematically in Appendices C and D, and in general TNNs allow arbitrary compound operation to be used at each linear layer.

One-layer of TNN We illustrate one layer of the Tensor-train TNN in Figure 4d (with input tensor of order $m = 5$), where the parameters are characterized by $(m - 1)$ kernels $\{\mathcal{K}_i\}_{i=0}^{m-2}$. The multi-dimensional structure lying in the higher-order input tensor \mathcal{U}' is effectively preserved: each mode i of the input tensor \mathcal{U}' contracts with the corresponding kernel \mathcal{K}_i . Tensor-train TNN allows interactions between the modes by the contraction edges between adjacent kernels \mathcal{K}_i and \mathcal{K}_{i+1} . These edges are crucial for modeling general multi-dimensional transformations while preserving the structures of the input data. Effectively, each layer of Tensor-train TNN implements a multi-dimensional propagation of the high-order input.

Relationship between TNNs and CNNs (1) *TNN generalizes NN*. Formally, for any $q > 0$, $\mathcal{G}^q \subseteq \mathcal{H}^q$ holds. Consider a special case of Figure 4d where \mathcal{K}_0 and \mathcal{K}_1 are identical mappings and contraction of \mathcal{K}_2 and \mathcal{K}_{m-2} equals to a kernel \mathcal{K} as in Figure 4c, the TNN reduces to a CNN. (2) *NN can be mapped to TNN with fewer parameters*. Formally, there exists $p \leq q$ such that $\mathcal{H}^p \subseteq \mathcal{G}^q$. Given an $h^p \in \mathcal{H}^p$, we could factorize \mathcal{K} into $\{\mathcal{K}_i\}_{i=0}^{m-2}$ using generalized tensor decomposition (as detailed in Section 4 and Appendix E), therefore find $q \leq p$ and $g^q \in \mathcal{G}^q$ ($\{\mathcal{K}_i\}_{i=0}^{m-2}$ altogether have fewer parameters than \mathcal{K}).

Why are TNNs more flexible than NNs? (1) TNNs are more flexible than NNs as the input can be tensors of arbitrary order, which naturally deals with data represented by multi-dimensional array without breaking their internal structures. (2) Even in the scenario that the input data is a vector or a matrix, one can reshape the input into higher-order tensor in order to exploit the invariant structures within the data discussed in Section 4.

3.2 Prediction in TNN

Prediction with a TNN proceeds similarly as a normal neural network: the input is passed through the layers in TNN in a feedforward manner, where each layer is a generalized tensor operation (multilinear operation) between the input and the model parameters followed by a nonlinear activation function such as ReLU. When the number of operands in a generalized

tensor operation is greater than two (i.e. the layer is characterized by more than one kernel), it is generally NP-hard to find the best order to evaluate the operation. We identify efficient strategies for all TNN architectures in this paper. For example, each layer in Tensor-train TNN can be efficiently evaluated as:

$$\mathcal{U}_{i+1} = \mathcal{U}^{(i)} (\times_1^2 \circ \times_0^{-1}) \mathcal{K}_i \quad (2a)$$

$$\mathcal{V}' = \mathcal{U}_{m-1} (*_1^0 \circ *_2^1 \circ \times_0^{-1}) \mathcal{K}_m \quad (2b)$$

where $\mathcal{U}_0 = \mathcal{U}'$ and \mathcal{V}' are the input/output of the layer, \mathcal{U}_i is the intermediate result after interacting with \mathcal{K}_i . The forward pass for other architectures are derived in Appendix G and H, with their complexities summarized in Table 1.

3.3 Learning in TNN

Learning in a TNN corresponds to *hierarchical nonlinear general tensor decomposition*, which recovers all tensors in the TNN. Solving the decomposition problem in closed form is difficult, therefore we derive the backpropagation rules for general tensor operations (in Appendix D) such that the tensors can be recovered by *stochastic gradient descent* approximately. For each layer in TNN, backpropagation requires computations of the derivatives of some loss function \mathcal{L} w.r.t. the input $\partial\mathcal{L}/\partial\mathcal{U}'$ and kernel factors $\{\partial\mathcal{L}/\partial\mathcal{K}_i\}_{i=0}^{m-2}$ given $\partial\mathcal{L}/\partial\mathcal{V}'$. As in forward pass, identifying the best strategy to compute these backpropagation equations simultaneously is NP-hard, and we need to develop efficient algorithm for each architecture. For the case of Tensor-train TNN, the algorithm proceeds as follows:

$$\frac{\partial\mathcal{L}}{\partial\mathcal{U}_{m-2}} = \frac{\partial\mathcal{L}}{\partial\mathcal{V}'} \left((*_1^0)^\top \circ (*_2^1)^\top \right) \mathcal{K}_{m-2} \quad (3a)$$

$$\frac{\partial\mathcal{L}}{\partial\mathcal{K}_{m-2}} = \frac{\partial\mathcal{L}}{\partial\mathcal{V}'} \left((*_0^0)^\top \circ (*_1^1)^\top \circ \times_2^2 \cdots \times_{m-1}^{m-1} \right) \mathcal{U}_{m-2} \quad (3b)$$

$$\frac{\partial\mathcal{L}}{\partial\mathcal{U}_i} = \text{swapaxes}(\mathcal{K}_i (\times_{-2}^2 \circ \times_{-1}^3) \frac{\partial\mathcal{L}}{\partial\mathcal{U}_{i+1}}) \quad (3c)$$

$$\frac{\partial\mathcal{L}}{\partial\mathcal{K}_i} = \text{swapaxes}(\mathcal{U}_i (\times_0^0 \circ \times_1^1 \circ \times_2^2 \cdots \times_{m-1}^{m-1}) \frac{\partial\mathcal{L}}{\partial\mathcal{U}_{i+1}}) \quad (3d)$$

where $\text{swapaxes}(\cdot)$ permutes the order as needed (explained in Appendix B). The algorithms for other architectures are derived in appendices G and H, whose time complexities are summarized in Table 1.

4 Compression of Neural Networks via TNN

Suppose we are given a pre-trained neural network $g^q \in \mathcal{G}^q$ with q parameters (as described in Figure 1) and we want to compress it to p parameters such that $p \ll q$. If we are looking for a compressed model in the class of traditional neural networks \mathcal{G}^p , any compression algorithm can at best find g^p , while if we consider a boarder class of compressed models in our proposed TNNs \mathcal{H}^p , a good enough compression algorithm finds $h^p \in \mathcal{H}^p \setminus \mathcal{G}^p$. As is demonstrated in Figure 1, h^p is closer to the uncompressed NN g^q than g^p , therefore outperforms g^p in its predictive accuracy.

We introduce a compression algorithm that projects a pre-trained NN $g \in \mathcal{G}^q$ to a TNN $h^* \in \mathcal{H}^p$. Superscripts on g and h are omitted for notational simplicity. Suppose the input to g is \mathcal{U} , our goal is to find a h^* such that

$$h^* = \arg \min_{h \in \mathcal{H}^p} \text{dist}(h(\mathcal{U}'), g(\mathcal{U})) \quad (4)$$

Architect.	$O(\# \text{ of parameters})$	$O(\# \text{ of forward ops.})$	$O(\# \text{ of backward ops.})$
original	$k^2 N^2$	$k^2 N^2 D^2$	$N^2 D^4$
TNN-mCP	$(k^2 + mN^{\frac{2}{m}})R$	$(mN^{1+\frac{1}{m}} + k^2 N)RD^2$	$(mN^{1+\frac{1}{m}} + ND^2)RD^2$
TNN-mTK	$(k^2 R^{2m-1} + 2mN)R$	$(k^2 R^{2m-1} + 2mN)RD^2$	$(R^{2m-1} D^2 + 2mN)RD^2$
TNN-mTT	$(mN^{\frac{2}{m}} R + k^2)R$	$(mN^{1+\frac{1}{m}} R + k^2 N)RD^2$	$(mN^{1+\frac{1}{m}} R + ND^2)RD^2$

Table 1: Number of parameters and operations required by one compressed convolutional layer using various types of tensor decompositions as the projection method. This table is for the special case when $X = Y = X' = Y' = D$, $S = T = N$, $H = W = k$ and $D \gg k$ (see equation 1). General settings are summarized in Tables 9 and 11.

where m -order \mathcal{U}' is the reshaped version of \mathcal{U} (to fit the input requirement of h), and $\text{dist}(\cdot, \cdot)$ denotes any distance, such as ℓ_2 distance, between the outputs of h and g .

4.1 Tensorization: Exploiting Invariant Structures

We first reshape the input data \mathcal{U} to m -order tensor \mathcal{U}' . Consider this toy example of a vector with periodic structure $[1, 2, 3, 1, 2, 3, 1, 2, 3]$ or modulated structure $[1, 1, 1, 2, 2, 2, 3, 3, 3]$ in Figure 5. The number of parameters needed to represent this vector, naively, is 9. However if we map or *reshape* the vector into a higher order object, for instance, a matrix ($m = 2$) $[1, 1, 1; 2, 2, 2; 3, 3, 3]$ where the columns of the matrix are repeated, then apparently this reshaped matrix can be decomposed into rank one without losing information. Therefore only 6 parameters are needed to represent the original length-9 vector.

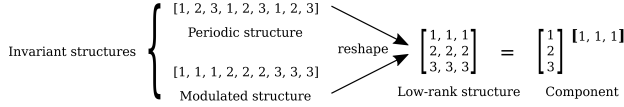


Figure 5: A toy example of invariant structures. The periodic and modulated structures are picked out by exploiting the low rank structure in the reshaped matrix.

Now we are ready to learn the mapping from NN to TNN.

4.2 Mapping NN to TNN

End-to-End (E2E) Learning Let the l -th layer of TNN h be parameterized by $(m - 1)$ kernels $\{\mathcal{K}_i^{(l)}\}_{i=0}^{m-2}$. if ℓ_2 distance is used, the compression reduces to an optimization problem :

$$\{\mathcal{K}_i^{(l)*}\}_{i,l} = \arg \min_{\{\mathcal{K}_i^{(l)}\}_{i,l}} \|h(\mathcal{U}') - g(\mathcal{U})\|_2^2 \quad (5)$$

Solving the problem by backpropagation is very expensive as it requires end-to-end gradients flow in TNN, therefore we relax it into a sequence of problems as follows.

Sequential (Seq) Learning Let $\mathcal{V}^{(l)}$ and $\mathcal{V}'^{(l)}$ be the outputs of the l -th layers of g and h . We propose to project each layer of g to a layer of h bottom-up sequentially, i.e. for $l = 0, \dots, L$:

$$\{\mathcal{K}_i^{(l)*}\}_i = \arg \min_{\{\mathcal{K}_i^{(l)}\}_i} \|\mathcal{V}^{(l)} - \mathcal{V}'^{(l)}\|_2^2 \quad (6)$$

where the input to these layers are fixed to $\mathcal{V}^{(l-1)}$ and $\mathcal{V}'^{(l-1)}$ respectively.

Generalized Tensor Decomposition Since each layer of TNN should approximate the pre-trained NN, our goal is to find $\mathcal{K}_i^{(l)*}$ such that their composition is closed to the uncompressed kernel $\mathcal{K}^{(l)}$, and in Tensor-train TNN:

$$\mathcal{K}^{(l)} \approx \mathcal{K}_0^{(l)*} \times_0^{-1} \mathcal{K}_1^{(l)*} \times_0^{-1} \dots \times_0^{-1} \mathcal{K}_{m-2}^{(l)*} \quad (7)$$

The equation above is known as *generalized tensor decomposition*, because it reverses the mapping of the general tensor operations proposed earlier: given a set of operations and a tensor, generalized tensor decomposition aims to recover the factors/components such that the operations on these factors result in a tensor approximately equal to the original one. (See Appendix E for details).

5 Interpretation of Neural Networks Designs

Recent advances in novel architecture design of neural networks include *Inception* [34], *Xception* [4] and *Bottleneck structures* [14, 25]. We will show, in this section, that all aforementioned architectures can be naturally derived as special cases of our TNN framework (with small modifications).

Inception Network. Inception network [34] is a special case of Tensor-train TNN as shown in Figure 6. For instance, an Inception network in Figure 6a can be represented using tensor diagram as in Figure 6b, a simplified Tensor-train TNN with input tensor of size 3×3 and the dimension of the connecting edge is 1.

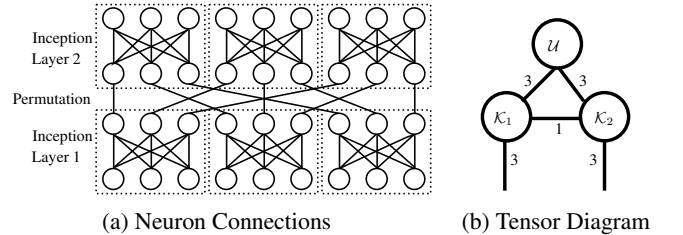


Figure 6: Inception networks.

Xception Network. Xception [4] is an architecture that further simplifies Inception, where local connection at the *depth-wise layers* are further limited to one neuron (or one feature map). Similar to Inception, the Xception network in Figure 7a can be represented using tensor diagram as in Figure 7b, a simple Tensor-train TNN with input tensor of size 2×2 and the dimension of the connecting edge is 2.

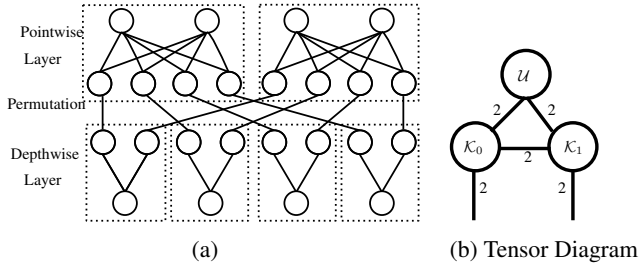


Figure 7: An Xception network.

Bottleneck Network. Finally, bottleneck architecture in [14, 25] can be interpreted as decomposition of a wider architecture into a tensor network with 3 kernels.

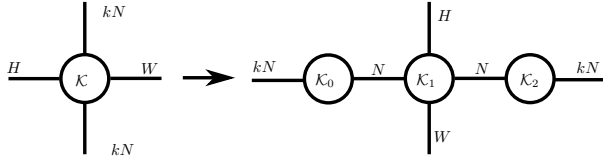


Figure 8: Bottleneck structure as tensor decomposition.

Insights for NN designs. Our TNN provides some insights on how to design a compact NN architecture in practice: (1) First, we can start our design with a traditional neural network (with wide architecture); (2) Second, we factorize the kernel into a tensor network by general tensor decomposition, which converts the original neural network into a TNN that naturally bear nice compact structures as we see in Figures 6a and 7a. (3) Since each tensor network corresponds to a compact design, therefore exploration of different designs can be done by designing different tensor networks.

6 Experiments

In this section, we evaluate the effectiveness of our proposed compression algorithm (TNN based compression) proposed in section 4 on several benchmark deep neural networks and datasets. We evaluate fully connected layer compression on MNIST (discussed in Appendix G); we evaluate convolutional layer compression on ResNet-32 [14] for CIFAR-10; and we evaluate the scalability of our compression algorithm on ResNet-50 [14] for ImageNet (2012) dataset.

We conduct experiments on various compression rates and compare the performance of our TNN based compression (TNN-C) methods with that of the state-of-the-art low-rank approximation based compression methods (NN-C [18, 19, 23]) under the same compression rate. More details of the state-of-the-art low-rank approximation based compression are provided in appendix F. For all experiments, we use the Adam optimizer [20] with $1e-3$ learning rate and decay the learning rate by 10x every 50 epochs. Overall, we show that our TNN based compression maintain high accuracy even when the networks are highly compressed.

We denote NN-CP, NN-TK, and NN-TT as the compressed neural network obtained by baseline low-rank approximation

based compression, which uses classical types of tensor decompositions (CP, TK, and TT) as the layer-wise projecting methods (mentioned in section 4). While TNN-mCP, TNN-mTK and TNN-mTT are compressed tensorial neural networks obtained by TNN based compression, which uses our proposed modified tensor decomposition (mCP, mTK, and mTT).

As mentioned in section 4, we refer to traditional back propagation-based compression of the network as end-to-end (E2E) compression, and refer to our strategy of data reconstruction-based sequential compression as Sequential (Seq) compression.

Our algorithm achieves 5% higher accuracy than baseline on CIFAR10 using ResNet-32. The results from table 2 demonstrate that our TNN-C maintains high accuracy even after the networks are highly compressed on CIFAR-10. Given a well-trained 32-layer ResNet network and a goal of reducing the number of parameters to 10% of the original size, the NN-CP obtained by NN-C using end-to-end compression reduces the original accuracy from 93.2% to 86.93%; while the TNN-mCP obtained by TNN-C paired with Seq compression increases the accuracy to 91.28% with the same compression rate — **a performance loss of 2% with only 10% of the number of parameters**. Furthermore, TNN-C achieves further aggressive compression — **a performance loss of 6% with only 2% of the number of parameters**. We observe similar trends (higher compression and higher accuracy) are observed for TNN-mTT as well. The structure of the Tucker decomposition (see section H) makes TNN-mTK less effective with very high compression, since the “internal structure” of the network reduces to very low rank, which may lose necessary information. Increasing the network size to 20% of the original provides reasonable performance on CIFAR-10 for TNN-mTK as well.

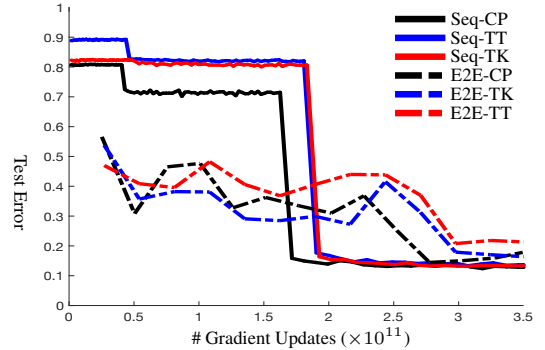


Figure 9: Convergence rate for Seq vs. E2E compression on CIFAR10.

Table 2 shows that *TNN-C with Seq compression* outperforms *NN-C with end-to-end compression*. Now we address the following question: is one factor (Seq compression or TNN-C) primarily responsible for increased performance, or is the benefit due to synergy between the two?

Seq compression, TNN based compression, or both? (1) We present the effect of different compression methods on accuracy in Table 3. Other than at very high compression rate

Architect.	Compression rate				Architect.	Compression rate			
	5%	10%	20%	40%		2%	5%	10%	20%
NN-SVD [18]	83.09	87.27	89.58	90.85	TNN-TR [†] [36]	-	80.80 [†]	-	90.60
NN-CP [23]	84.02	86.93	88.75	88.75	TNN-mCP	85.7	89.86	91.28	-
NN-TK [19]	83.57	86.00	88.03	89.35	TNN-mTK	61.06	71.34	81.59	87.11
NN-TT	77.44	82.92	84.13	86.64	TNN-mTT	78.95	84.26	87.89	-

[†]The tensor ring (TR) results are cited from [36], and the accuracy of 80.8% is achieved by 6.67% compression rate.

Table 2: Percentage test accuracy of baseline **NN-C** with E2E compression vs. our **TNN-C** with Seq compression on CIFAR10. The uncompressed ResNet-32 achieves 93.2% accuracy with 0.46M parameters.

Architect.	Compression rate							
	5%		10%		20%		40%	
	Seq	E2E	Seq	E2E	Seq	E2E	Seq	E2E
NN-SVD	74.04	83.09	85.28	87.27	89.74	89.58	91.83	90.85
NN-CP	83.19	84.02	88.50	86.93	90.72	88.75	89.75	88.75
NN-TK	80.11	83.57	86.75	86.00	89.55	88.03	91.3	89.35
NN-TT	80.77	77.44	87.08	82.92	89.14	84.13	91.21	86.64

Table 3: Percentage accuracy of **our Seq** vs. **baseline E2E** tuning using NN-C on CIFAR10.

Architect.	Compression rate		Architect.	Compression rate	
	5%	10%		5%	10%
NN-CP	83.19	88.50	TNN-mCP	89.86	91.28
NN-TK	80.11	86.73	TNN-mTK	71.34	81.59
NN-TT	80.77	87.08	TNN-mTT	84.26	87.89

Table 4: Percentage accuracy of **our TNN-C** vs. **baseline NN-C** using Seq tuning on CIFAR10.

# epochs	# samples	Uncompressed # params. = 25M	NN-TT (E2E) # params. = 2.5M	TNN-mTT (Seq) # params. = 2.5M
0.2	0.24M	4.22	2.78	44.35
0.3	0.36M	6.23	3.99	46.98
0.5	0.60M	9.01	7.48	49.92
1.0	1.20M	17.3	12.80	52.59
2.0	2.40M	30.8	18.17	54.00

Table 5: Convergence of percentage accuracies of **uncompressed** vs. **NN-C** (TT decomposition) vs. **TNN-C** (TNN-mTT decomposition) achieving 10% compression rate for ResNet-50 ImageNet.

(5% column in Table 3), Seq compression (Seq) consistently outperforms end-to-end (E2E) compression. In addition, Seq compression is also *much* faster and leads to more stable convergence compared to end-to-end compression. Figure 9 plots the compression error over the number of gradient updates for various compression methods. (2) We present the effect of different compression methods on accuracy in Table 4. Interestingly, as what is demonstrated in Table 4, if TNN based compression method is used, the test accuracy is restored for even very high compression ratios¹. These results confirm that TNN is more flexible than NN as TNN allows exploitation of additional invariant structures in the parameter space of deep neural networks, and such invariant structures are picked up by our proposed TNN based compression (our TNN-C), but not by low-rank approximation based compression (NN-C). Therefore, our results show that TNN-C and Seq compression are symbiotic, and *both* are necessary to simultaneously obtain a high accuracy and a high compression rate.

Scalability Finally, we show that our methods scale to state-of-the-art large networks, by evaluating performance on the ImageNet 2012 dataset on a 50-layer ResNet (uncompressed with 76.05% accuracy). Table 5 shows the accuracy of TNN-mTT obtained by TNN-C with Seq tuning compared to that of NN-TT obtained by low-rank approximation based compression with E2E tuning, and the accuracy of the uncompressed network (ResNet-50) with 10% compression rate. Table 5 shows that TNN-C paired with Seq tuning is much faster than the alternative. This is an important result because it empirically validates our hypotheses that (1) our TNN based compression captures the invariant structure of the ResNet (with few redundancies) better and faster than the baseline NN-C compression, (2) data reconstruction Seq tuning is effective even on the largest networks and datasets, and (3) our proposed efficient TNN-C can scale to the state-of-the-art neural networks.

7 Conclusion and Perspectives

We define a new generalized tensor algebra extending existing tensor operations. We extend vector/matrix operations to their higher order tensor counterparts, providing systematic notations and libraries for tensorization of neural networks and higher order tensor decompositions. Using these generalized tensor operations, we introduce tensorial neural networks (TNN) which extends existing neural networks. Our TNN is more flexible than NN and more compact than neural networks allowing same amount expressive power with fewer number of parameters. Therefore mapping NN to its closest TNN is a compression of NN as the resulting TNN will carry fewer number of parameters. Other compression techniques as mentioned in the related work can naturally be used on the compressed TNN to further compress the TNN. As a future step, we will explore optimizing the order of (parallel) implementations of the tensor algebra.

¹Note that TNN-mTK remains an exception for aggressive compression due to the low rank internal structure that we previously discussed.

References

- [1] Jimmy Ba and Rich Caruana. Do deep nets really need to be deep? In *Advances in neural information processing systems*, pages 2654–2662, 2014.
- [2] Yu Cheng, Felix X Yu, Rogerio S Feris, Sanjiv Kumar, Alok Choudhary, and Shi-Fu Chang. An exploration of parameter redundancy in deep networks with circulant projections. In *Proceedings of the IEEE International Conference on Computer Vision*, pages 2857–2865, 2015.
- [3] Yu Cheng, Duo Wang, Pan Zhou, and Tao Zhang. A survey of model compression and acceleration for deep neural networks. *arXiv preprint arXiv:1710.09282*, 2017.
- [4] François Chollet. Xception: Deep learning with depthwise separable convolutions. *arXiv preprint arXiv:1610.02357*, 2016.
- [5] Andrzej Cichocki, Namgil Lee, Ivan V Oseledets, Anh Huy Phan, Qibin Zhao, and D Mandic. Low-rank tensor networks for dimensionality reduction and large-scale optimization problems: Perspectives and challenges part 1. *arXiv preprint arXiv:1609.00893*, 2016.
- [6] Andrzej Cichocki, Anh-Huy Phan, Qibin Zhao, Namgil Lee, Ivan Oseledets, Masashi Sugiyama, Danilo P Mandic, et al. Tensor networks for dimensionality reduction and large-scale optimization: Part 2 applications and future perspectives. *Foundations and Trends® in Machine Learning*, 9(6):431–673, 2017.
- [7] Pierre Comon, Xavier Luciani, and André LF De Almeida. Tensor decompositions, alternating least squares and other tales. *Journal of Chemometrics: A Journal of the Chemometrics Society*, 23(7-8):393–405, 2009.
- [8] Matthieu Courbariaux, Yoshua Bengio, and Jean-Pierre David. Binaryconnect: Training deep neural networks with binary weights during propagations. In *Advances in neural information processing systems*, pages 3123–3131, 2015.
- [9] Emily L Denton, Wojciech Zaremba, Joan Bruna, Yann LeCun, and Rob Fergus. Exploiting linear structure within convolutional networks for efficient evaluation. In *Advances in neural information processing systems*, pages 1269–1277, 2014.
- [10] Tommaso Furlanello, Zachary C Lipton, Michael Tschannen, Laurent Itti, and Anima Anandkumar. Born again neural networks. *arXiv preprint arXiv:1805.04770*, 2018.
- [11] Lars Grasedyck, Daniel Kressner, and Christine Tobler. A literature survey of low-rank tensor approximation techniques. *GAMM-Mitteilungen*, 36(1):53–78, 2013.
- [12] Song Han, Huizi Mao, and William J Dally. Deep compression: Compressing deep neural networks with pruning, trained quantization and huffman coding. *arXiv preprint arXiv:1510.00149*, 2015.
- [13] Kaiming He, Xiangyu Zhang, Shaoqing Ren, and Jian Sun. Deep residual learning for image recognition. In

- Proceedings of the IEEE conference on computer vision and pattern recognition*, pages 770–778, 2016.
- [14] Kaiming He, Xiangyu Zhang, Shaoqing Ren, and Jian Sun. Identity mappings in deep residual networks. In *European Conference on Computer Vision*, pages 630–645. Springer, 2016.
- [15] Geoffrey Hinton, Oriol Vinyals, and Jeff Dean. Distilling the knowledge in a neural network. *arXiv preprint arXiv:1503.02531*, 2015.
- [16] Gao Huang, Zhuang Liu, Laurens Van Der Maaten, and Kilian Q Weinberger. Densely connected convolutional networks. In *CVPR*, volume 1, page 3, 2017.
- [17] Itay Hubara, Matthieu Courbariaux, Daniel Soudry, Ran El-Yaniv, and Yoshua Bengio. Quantized neural networks: Training neural networks with low precision weights and activations. *Journal of Machine Learning Research*, 18:187–1, 2017.
- [18] Max Jaderberg, Andrea Vedaldi, and Andrew Zisserman. Speeding up convolutional neural networks with low rank expansions. *arXiv preprint arXiv:1405.3866*, 2014.
- [19] Yong-Deok Kim, Eunhyeok Park, Sungjoo Yoo, Taelim Choi, Lu Yang, and Dongjun Shin. Compression of deep convolutional neural networks for fast and low power mobile applications. *arXiv preprint arXiv:1511.06530*, 2015.
- [20] Diederik P Kingma and Jimmy Ba. Adam: A method for stochastic optimization. *arXiv preprint arXiv:1412.6980*, 2014.
- [21] Tamara G Kolda and Brett W Bader. Tensor decompositions and applications. *SIAM review*, 51(3):455–500, 2009.
- [22] Alex Krizhevsky, Ilya Sutskever, and Geoffrey E Hinton. Imagenet classification with deep convolutional neural networks. In *Advances in neural information processing systems*, pages 1097–1105, 2012.
- [23] Vadim Lebedev, Yaroslav Ganin, Maksim Rakhuba, Ivan Oseledets, and Victor Lempitsky. Speeding-up convolutional neural networks using fine-tuned cp-decomposition. *arXiv preprint arXiv:1412.6553*, 2014.
- [24] Yann LeCun, Léon Bottou, Yoshua Bengio, and Patrick Haffner. Gradient-based learning applied to document recognition. *Proceedings of the IEEE*, 86(11):2278–2324, 1998.
- [25] Min Lin, Qiang Chen, and Shuicheng Yan. Network in network. *arXiv preprint arXiv:1312.4400*, 2013.
- [26] Alexander Novikov, Dmitrii Podoprikin, Anton Osokin, and Dmitry P Vetrov. Tensorizing neural networks. In *Advances in Neural Information Processing Systems*, pages 442–450, 2015.
- [27] Román Orús. A practical introduction to tensor networks: Matrix product states and projected entangled pair states. *Annals of Physics*, 349:117–158, 2014.
- [28] Ivan V Oseledets. Tensor-train decomposition. *SIAM Journal on Scientific Computing*, 33(5):2295–2317, 2011.
- [29] Mohammad Rastegari, Vicente Ordonez, Joseph Redmon, and Ali Farhadi. Xnor-net: Imagenet classification using binary convolutional neural networks. In *European Conference on Computer Vision*, pages 525–542. Springer, 2016.
- [30] Adriana Romero, Nicolas Ballas, Samira Ebrahimi Kahou, Antoine Chassang, Carlo Gatta, and Yoshua Bengio. Fitnets: Hints for thin deep nets. *arXiv preprint arXiv:1412.6550*, 2014.
- [31] Karen Simonyan and Andrew Zisserman. Very deep convolutional networks for large-scale image recognition. *arXiv preprint arXiv:1409.1556*, 2014.
- [32] Vikas Sindhwani, Tara Sainath, and Sanjiv Kumar. Structured transforms for small-footprint deep learning. In *Advances in Neural Information Processing Systems*, pages 3088–3096, 2015.
- [33] Christian Szegedy, Wei Liu, Yangqing Jia, Pierre Sermanet, Scott Reed, Dragomir Anguelov, Dumitru Erhan, Vincent Vanhoucke, and Andrew Rabinovich. Going deeper with convolutions. In *Proceedings of the IEEE conference on computer vision and pattern recognition*, pages 1–9, 2015.
- [34] Christian Szegedy, Sergey Ioffe, Vincent Vanhoucke, and Alexander A Alemi. Inception-v4, inception-resnet and the impact of residual connections on learning. In *AAAI*, volume 4, page 12, 2017.
- [35] Po-An Wang and Chi-Jen Lu. Tensor decomposition via simultaneous power iteration. In *International Conference on Machine Learning*, pages 3665–3673, 2017.
- [36] Wenqi Wang, Yifan Sun, Brian Eriksson, Wenlin Wang, and Vaneet Aggarwal. Wide compression: Tensor ring nets. *learning*, 14(15):13–31, 2018.
- [37] Zichao Yang, Marcin Moczulski, Misha Denil, Nando de Freitas, Alex Smola, Le Song, and Ziyu Wang. Deep fried convnets. In *Proceedings of the IEEE International Conference on Computer Vision*, pages 1476–1483, 2015.
- [38] Chenzhuo Zhu, Song Han, Huizi Mao, and William J Dally. Trained ternary quantization. *arXiv preprint arXiv:1612.01064*, 2016.

Appendix: Tensorial Neural Networks: Generalization of Neural Networks and Application to Model Compression

A Supplementary experiments

Convergence Rate Compared to end-to-end, an ancillary benefit of sequential tuning is *much* faster and leads to more stable convergence. Figure 9 plots compression error over number of gradient updates for various methods. (This experiment is for NN-C with 10% compression rate.) There are three salient points: first, sequential tuning has very high error in the beginning while the "early" blocks of the network are being tuned (and the rest of the network is left unchanged to tensor decomposition values). However, as the final block is tuned (around 2×10^{11} gradient updates) in the figure, the errors drop to nearly minimum immediately. In comparison, end-to-end tuning requires 50–100% more gradient updates to achieve stable performance. Finally, the result also shows that for each block, sequential tuning achieves convergence very quickly (and nearly monotonically), which results in the stair-step pattern since extra tuning of a block does not improve (or appreciably reduce) performance.

Performance on Fully-Connected Layers An extra advantage of TNN based compression is that it can apply flexibly to fully-connected as well as convolutional layers of a neural network. Table 6 shows the results of applying TNN based compression to various tensor decompositions on a variant of LeNet-5 network [24]. The convolutional layers of the LeNet-5 network were *not* compressed, trained or updated in these experiments. The uncompressed network achieves 99.31% accuracy. Table 6 shows **the fully-connected layers can be compressed to 0.2% losing only about 2% accuracy**. In fact, compressing the dense layers to 1% of their original size reduce accuracy by less than 1%, demonstrating the extreme efficacy of TNN based compression when applied to fully-connected neural network layers.

Architect.	Compression rate		
	0.2%	0.5%	1%
TNN-mCP	97.21	97.92	98.65
TNN-mTK	97.71	98.56	98.52
TNN-mTT	97.69	98.43	98.63

Table 6: TNN compression of fully-connected layer in LeNet-5. The uncompressed network achieves 99.31% accuracy.

B Notations

Symbols: Lower case letters (e.g. \mathbf{v}) are used to denote column vectors, while upper case letters (e.g. \mathbf{M}) are used for matrices, and curled letters (e.g. \mathcal{T}) for multi-dimensional arrays (tensors). For a tensor $\mathcal{T} \in \mathbb{R}^{I_0 \times \dots \times I_{m-1}}$, we will refer to the number of indices as *order*, each individual index as *mode* and the length at one mode as *dimension*. Therefore, we will say that $\mathcal{T} \in \mathbb{R}^{I_0 \times \dots \times I_{m-1}}$ is an m -order tensor which has dimension I_k at mode- k . *Tensor operations* are extensively used in this paper: The *tensor (partial) outer product* is denoted as \otimes , *tensor convolution* as $*$, and finally \times denotes either *tensor contraction* or *tensor multiplication*. Each of these operators will be equipped with subscript and superscript when used in practice, for example \times_n^m denotes mode- (m, n) tensor contraction (defined in Appendix C). Furthermore, the symbol \circ is used to construct *compound operations*. For example, $(* \circ \otimes)$ is a compound operator simultaneously performing tensor convolution and tensor partial outer product between two tensors.

Indexing: In this paragraph, we explain the usages of subscripts/superscripts for both multi-dimensional arrays and operators, and further introduce several functions that are used to alter the layout of multi-dimensional arrays.

- (1) Nature indices start from 0, but reversed indices are used occasionally, which start from -1 . Therefore the first entry of a vector \mathbf{v} is v_0 , while the last one is v_{-1} . (2) For multi-dimensional arrays, the *subscript* is used to denote an entry or a subarray within an object, while *superscript* is to index among a sequence of arrays. For example, $\mathbf{M}_{i,j}$ denotes the entry at i^{th} row and j^{th} column of a matrix \mathbf{M} , and $\mathbf{M}^{(k)}$ is the k^{th} matrix in a set of N matrices $\{\mathbf{M}^{(0)}, \mathbf{M}^{(1)}, \dots, \mathbf{M}^{(N-1)}\}$. For operators, as we have seen, both subscript and superscript are used to denote the modes involved in the operation. (3) The *symbol colon* ':' is used to slice a multi-dimensional array. For example, $\mathcal{M}_{:,k}$ denotes the k^{th} column of \mathbf{M} , and $\mathcal{T}_{:,:,k}$ denotes the k^{th} *frontal slice* of a 3-order tensor \mathcal{T} . (4) *Big-endian notation* is adopted in conversion between multi-dimensional array and vectors. Specifically, the function $\text{vec}(\cdot)$ flattens (a.k.a. *vectorize*) a tensor $\mathcal{T} \in \mathbb{R}^{I_0 \times \dots \times I_{m-1}}$ into a vector $\mathbf{v} \in \mathbb{R}^{\prod_{i=0}^{m-1} I_i}$ such that $\mathcal{T}_{i_0, \dots, i_{m-1}} = v_{i_{m-1} + i_{m-2}I_{m-1} + \dots + i_0 I_1 \dots I_{m-1}}$.
- (1) The function $\text{swapaxes}(\cdot)$ is used to permute ordering of the modes of a tensor as needed. For example, given two tensors $\mathcal{U} \in \mathbb{R}^{I \times J \times K}$ and $\mathcal{V} \in \mathbb{R}^{K \times J \times I}$, the operation $\mathcal{V} = \text{swapaxes}(\mathcal{U})$ convert the tensor \mathcal{U} into \mathcal{V} such that $\mathcal{V}_{k,j,i} = \mathcal{U}_{i,j,k}$. (2) The function $\text{flipaxis}(\cdot, \cdot)$ flips a tensor along a given mode. For example, given a tensor $\mathcal{U} \in \mathbb{R}^{I \times J \times K}$ and $\mathcal{V} = \text{flipaxis}(\mathcal{U}, 0)$, the entries in \mathcal{V} is defined as $\mathcal{V}_{i,j,k} = \mathcal{U}_{I-1-i(\text{mod } I),j,k}$.

C Tensor operations

Operator	Notation	Definition
mode- (k, l) Tensor Contraction	$\mathcal{T}^{(0)} = \mathcal{X} \times_l^k \mathcal{Y}$	$\mathcal{T}_{i_0, \dots, i_{k-1}, i_{k+1}, \dots, i_{m-1}, j_0, \dots, j_{l-1}, j_{l+1}, \dots, j_{n-1}}^{(0)}$ $= \langle \mathcal{X}_{i_0, \dots, i_{k-1}, :, i_{k+1}, \dots, i_{m-1}}, \mathcal{Y}_{j_0, \dots, j_{l-1}, :, j_{l+1}, \dots, j_{n-1}} \rangle$ inner product of mode- k fiber of \mathcal{X} and mode- l fiber of \mathcal{Y}
mode- k Tensor Multiplication	$\mathcal{T}^{(1)} = \mathcal{X} \times_k \mathbf{M}$	$\mathcal{T}_{i_0, \dots, i_{k-1}, r, i_{k+1}, \dots, i_{m-1}}^{(1)}$ $= \langle \mathcal{X}_{i_0, \dots, i_{k-1}, :, i_{k+1}, \dots, i_{m-1}}, \mathbf{M}_{:,r} \rangle$ inner product of mode- k fiber of \mathcal{X} and r^{th} column of \mathbf{M}
mode- (k, l) Tensor Convolution	$\mathcal{T}^{(2)} = \mathcal{X} *_l^k \mathcal{Y}$	$\mathcal{T}_{i_0, \dots, i_{k-1}, :, i_{k+1}, \dots, i_{m-1}, j_0, \dots, j_{l-1}, j_{l+1}, \dots, j_{n-1}}^{(2)}$ $= \mathcal{X}_{i_0, \dots, i_{k-1}, :, i_{k+1}, \dots, i_{m-1}} * \mathcal{Y}_{j_0, \dots, j_{l-1}, :, j_{l+1}, \dots, j_{n-1}}$ convolution of mode- k fiber of \mathcal{X} and mode- l fiber of \mathcal{Y}
mode- (k, l) Partial- Outer Product	$\mathcal{T}^{(3)} = \mathcal{X} \otimes_l^k \mathcal{Y}$	$\mathcal{T}_{i_0, \dots, i_{k-1}, r, i_{k+1}, \dots, i_{m-1}, j_0, \dots, j_{n-1}}^{(3)}$ $= \mathcal{X}_{i_0, \dots, i_{k-1}, r, i_{k+1}, \dots, i_{m-1}} \mathcal{Y}_{j_0, \dots, j_{l-1}, r, j_{l+1}, \dots, j_{n-1}}$ Hadamard product of mode- k fiber of \mathcal{X} and mode- l fiber of \mathcal{Y}

Table 7: **Summary of tensor operations.** In this table, $\mathcal{X} \in \mathbb{R}^{I_0 \times \dots \times I_{m-1}}$, $\mathcal{Y} \in \mathbb{R}^{J_0 \times \dots \times J_{n-1}}$ and matrix $\mathbf{M} \in \mathbb{R}^{I_k \times J}$. Mode- (k, l) tensor contraction and mode- (k, l) tensor partial-outer product are legal only if $I_k = J_l$. $\mathcal{T}^{(0)}$ is an $(m + n - 2)$ -order tensor, $\mathcal{T}^{(1)}$ is an m -order tensor, $\mathcal{T}^{(2)}$ is an $(m + n - 1)$ -order tensor and $\mathcal{T}^{(3)}$ is an $(m + n - 1)$ -order tensor.

To begin with, we describe several *basic tensor operations* that are natural generalization to their vector/matrix counterparts. These basic operations can be further combined to construct *compound operations* that serve as building blocks of *tensorial neural networks*.

Tensor contraction Given an m -order tensor $\mathcal{T}^{(0)} \in \mathbb{R}^{I_0 \times \dots \times I_{m-1}}$ and another n -order tensor $\mathcal{T}^{(1)} \in \mathbb{R}^{J_0 \times \dots \times J_{n-1}}$, which share the same dimension at mode- k of $\mathcal{T}^{(0)}$ and mode- l of $\mathcal{T}^{(1)}$ (i.e. $I_k = J_l$), the mode- (k, l) contraction of $\mathcal{T}^{(0)}$ and $\mathcal{T}^{(1)}$, denoted as $\mathcal{T} \triangleq \mathcal{T}^{(0)} \times_l^k \mathcal{T}^{(1)}$, returns a $(m + n - 2)$ -order tensor $\mathcal{T} \in \mathbb{R}^{I_0 \times \dots \times I_{k-1} \times I_{k+1} \times \dots \times I_{m-1} \times J_0 \times \dots \times J_{l-1} \times J_{l+1} \times \dots \times J_{n-1}}$, whose entries are computed as

$$\begin{aligned} & \mathcal{T}_{i_0, \dots, i_{k-1}, i_{k+1}, \dots, i_{m-1}, j_0, \dots, j_{l-1}, j_{l+1}, \dots, j_{n-1}} \\ &= \sum_{r=0}^{I_k-1} \mathcal{T}_{i_0, \dots, i_{k-1}, r, i_{k+1}, \dots, i_{m-1}}^{(0)} \mathcal{T}_{j_0, \dots, j_{l-1}, r, j_{l+1}, \dots, j_{n-1}}^{(1)} \end{aligned} \quad (8a)$$

$$= \langle \mathcal{T}_{i_0, \dots, i_{k-1}, :, i_{k+1}, \dots, i_{m-1}}^{(0)}, \mathcal{T}_{j_0, \dots, j_{l-1}, :, j_{l+1}, \dots, j_{n-1}}^{(1)} \rangle \quad (8b)$$

Notice that tensor contraction is a direct generalization of matrix multiplication to higher-order tensor, and it reduces to matrix multiplication if both tensors are 2-order (and therefore matrices). As each entry in \mathcal{T} can be computed as inner product of two vectors, which requires $I_k = J_l$ multiplications, the total number of operations to evaluate a tensor contraction is therefore $O((\prod_{u=0}^{m-1} I_u)(\prod_{v=0, v \neq l}^{n-1} J_v))$, taking additions into account.

Tensor multiplication (Tensor product) Tensor multiplication (a.k.a. tensor product) is a special case of tensor contraction where the second operand is a matrix. Given a m -order tensor $\mathcal{U} \in \mathbb{R}^{I_0 \times \dots \times I_{m-1}}$ and a matrix $\mathbf{M} \in \mathbb{R}^{I_k \times J}$, where the dimension of \mathcal{U} at mode- k agrees with the number of the rows in \mathbf{M} , the mode- k tensor multiplication of \mathcal{U} and \mathbf{M} , denoted as $\mathcal{V} \triangleq \mathcal{U} \times_k \mathbf{M}$, yields another m -order tensor $\mathcal{V} \in \mathbb{R}^{I_0 \times \dots \times I_{k-1} \times J \times I_{k+1} \times \dots \times I_{m-1}}$, whose entries are computed as

$$\begin{aligned} & \mathcal{V}_{i_0, \dots, i_{k-1}, j, i_{k+1}, \dots, i_{m-1}} \\ &= \sum_{r=0}^{I_k-1} \mathcal{U}_{i_0, \dots, i_{k-1}, r, i_{k+1}, \dots, i_{m-1}} \mathbf{M}_{r,j} \end{aligned} \quad (9a)$$

$$= \langle \mathcal{U}_{i_0, \dots, i_{k-1}, :, i_{k+1}, \dots, i_{m-1}}, \mathbf{M}_{:,j} \rangle \quad (9b)$$

Following the convention of multi-linear algebra, the mode for J now substitutes the location originally for I_k (which is different from the definition of tensor contraction). Regardless, the number of operations for tensor multiplication follows tensor contraction exactly, that is $O((\prod_{u=0}^{m-1} I_u)J)$.

Tensor convolution Given a m -order tensor $\mathcal{T}^{(0)} \in \mathbb{R}^{I_0 \times I_1 \times \dots \times I_{m-1}}$ and another n -order tensor $\mathcal{T}^{(1)} \in \mathbb{R}^{J_0 \times J_1 \times \dots \times J_{n-1}}$. The mode- (k, l) convolution of $\mathcal{T}^{(0)}$ and $\mathcal{T}^{(1)}$, denoted as $\mathcal{T} \triangleq \mathcal{T}^{(0)} *_l^k \mathcal{T}^{(1)}$, returns a $(m+n-1)$ -order tensor $\mathcal{T} \in \mathbb{R}^{I_0 \times \dots \times I'_k \times \dots \times I_{m-1} \times J_0 \times \dots \times J_{l-1} \times J_{l+1} \times \dots \times J_{n-1}}$. The entries of \mathcal{T} can be computed using any convolution operation $*$ that is defined for two vectors.

$$\begin{aligned} & \mathcal{T}_{i_0, \dots, i_{k-1}, :, i_{k+1}, \dots, i_{m-1}, j_0, \dots, j_{l-1}, j_{l+1}, \dots, j_{n-1}} \\ &= \mathcal{T}_{i_0, \dots, i_{k-1}, :, i_{k+1}, \dots, i_{m-1}}^{(0)} * \mathcal{T}_{j_0, \dots, j_{l-1}, :, j_{l+1}, \dots, j_{n-1}}^{(1)} \end{aligned} \quad (10a)$$

$$= \mathcal{T}_{j_0, \dots, j_{l-1}, :, j_{l+1}, \dots, j_{n-1}}^{(1)} \bar{*} \mathcal{T}_{i_0, \dots, i_{k-1}, :, i_{k+1}, \dots, i_{m-1}}^{(0)} \quad (10b)$$

Here we deliberately omit the exact definition of vector convolution $*$ (and its conjugate $\bar{*}$), because it can be defined differently depending on the user case (Interestingly, the "convolution" in convolutional layer indeed computes *correlation* instead of convolution). Correspondingly, the resulted dimension I'_k at mode- k is determined by the chosen type of convolution. For example, the "convolution" in convolutional layer typically yields $I'_k = I_k$ (with same padding) or $I'_k = I_k - J_l + 1$ (with valid padding). Without *Fast Fourier Transform (FFT)*, the number of operations is $O((\prod_{u=0}^{m-1} I_u)(\prod_{v=0}^{n-1} J_v))$.

Tensor outer product Given a m -order tensor $\mathcal{T}^{(0)} \in \mathbb{R}^{I_0 \times I_1 \times \dots \times I_{m-1}}$ and another n -order tensor $\mathcal{T}^{(1)} \in \mathbb{R}^{J_0 \times J_1 \times \dots \times J_{n-1}}$, the outer product of $\mathcal{T}^{(0)}$ and $\mathcal{T}^{(1)}$, denoted $\mathcal{T} \triangleq \mathcal{T}^{(0)} \otimes \mathcal{T}^{(1)}$, concatenates all the indices of $\mathcal{T}^{(0)}$ and $\mathcal{T}^{(1)}$, and returns a $(m+n)$ -order tensor $\mathcal{T} \in \mathbb{R}^{I_0 \times \dots \times I_{m-1} \times J_0 \times \dots \times J_{n-1}}$ whose entries are computed as

$$\mathcal{T}_{i_0, \dots, i_{m-1}, j_0, \dots, j_{n-1}} = \mathcal{T}_{i_0, \dots, i_{m-1}}^{(0)} \mathcal{T}_{j_0, \dots, j_{n-1}}^{(1)} \quad (11)$$

It is not difficult to see that tensor outer product is a direct generalization for outer product for two vectors $\mathbf{M} = \mathbf{u} \otimes \mathbf{v} = \mathbf{u} \mathbf{v}^\top$. Obviously, the number of operations to compute a tensor outer product explicitly is $O((\prod_{u=0}^{m-1} I_u)(\prod_{v=0}^{n-1} J_v))$.

Tensor partial outer product Tensor partial outer product is a variant of tensor outer product defined above, which is widely used in conjunction with other operations. Given a m -order tensor $\mathcal{T}^{(0)} \in \mathbb{R}^{I_0 \times I_1 \times \dots \times I_{m-1}}$ and another n -order tensor $\mathcal{T}^{(1)} \in \mathbb{R}^{J_0 \times J_1 \times \dots \times J_{n-1}}$, which share the same dimension at mode- k of $\mathcal{T}^{(0)}$ and mode- l of $\mathcal{T}^{(1)}$ (i.e. $I_k = J_l$), the mode- (k, l) partial outer product of $\mathcal{T}^{(0)}$ and $\mathcal{T}^{(1)}$, denoted as $\mathcal{T} \triangleq \mathcal{T}^{(0)} \otimes_l^k \mathcal{T}^{(1)}$, returns a $(m+n-1)$ -order tensor $\mathcal{T} \in \mathbb{R}^{I_0 \times \dots \times I_{m-1} \times J_0 \times \dots \times J_{l-1} \times J_{l+1} \times \dots \times J_{n-1}}$, whose entries are computed as

$$\begin{aligned} & \mathcal{T}_{i_0, \dots, i_{k-1}, r, i_{k+1}, \dots, i_{m-1}, j_0, \dots, j_{l-1}, j_{l+1}, \dots, j_{n-1}} \\ &= \mathcal{T}_{i_0, \dots, i_{k-1}, r, i_{k+1}, \dots, i_{m-1}}^{(0)} \mathcal{T}_{j_0, \dots, j_{l-1}, r, j_{l+1}, \dots, j_{n-1}}^{(1)} \end{aligned} \quad (12a)$$

$$= \mathcal{T}_{\dots, r, \dots}^{(0)} \otimes \mathcal{T}_{\dots, r, \dots}^{(1)} \quad (12b)$$

The operation bears the name "partial outer product" because it reduces to outer product once we fix the indices at mode- k of $\mathcal{T}^{(0)}$ and mode- l of $\mathcal{T}^{(1)}$. Referring to the computational complexity of tensor outer product, the number of operations for each fixed index is $O((\prod_{u=0, u \neq k}^{m-1} I_u)(\prod_{v=0, v \neq l}^{n-1} J_v))$, therefore the total time complexity for the tensor partial outer product is $O((\prod_{u=0}^{m-1} I_u)(\prod_{v=0, v \neq l}^{n-1} J_v))$.

Compound operations: As building blocks, the basic tensor operations defined above can further combined to construct compound operations that perform multiple operations on multiple tensors simultaneously. We illustrate their usage using two representative examples in this section, and we will see more examples when we derive backpropagation rules for tensor operations in Appendix D.

- **Simultaneous multi-operations between two tensors.** For example, given two 3-order tensors $\mathcal{T}^{(0)} \in \mathbb{R}^{R \times X \times S}$ and $\mathcal{T}^{(1)} \in \mathbb{R}^{R \times H \times S}$, we can define a compound operation $(\otimes_0^0 \circ * \otimes_1^1 \circ \times_2^2)$ between $\mathcal{T}^{(0)}$ and $\mathcal{T}^{(1)}$, where mode- $(0, 0)$ partial outer product, mode- $(1, 1)$ convolution and mode- $(2, 2)$ contraction are performed simultaneously, which results in a 2-order tensor \mathcal{T} of $\mathbb{R}^{R \times X'}$ (it is indeed a matrix, though denoted as a tensor). The entries of $\mathcal{T} \triangleq \mathcal{T}^{(0)} (\otimes_0^0 \circ * \otimes_1^1 \circ \times_2^2) \mathcal{T}^{(1)}$ are computed as

$$\mathcal{T}_{r, :} = \sum_{s=0}^{S-1} \mathcal{T}_{r, :, s}^{(0)} * \mathcal{T}_{r, :, s}^{(1)} \quad (13)$$

For commonly used vector convolution, it is not difficult to show that number of operations required to compute the result \mathcal{T} is $O(R \max(X, H) \log(\max(X, H))S)$ with FFT and $O(RXH S)$ without FFT, as each of the R vectors in \mathcal{T} is computed with a sum of S vector convolutions.

- **Simultaneous operations between a tensor and a set of multiple tensors.** For example, given a 3-order tensor $\mathcal{U} \in \mathbb{R}^{R \times X \times S}$ and a set of three tensors $\mathcal{T}^{(0)} \in \mathbb{R}^{R \times P}$, $\mathcal{T}^{(1)} \in \mathbb{R}^{K \times Q}$ and $\mathcal{T}^{(2)} \in \mathbb{R}^{S \times T}$, we can define a compound operation on

\mathcal{U} as $\mathcal{V} \triangleq \mathcal{U}(\otimes_0^0 \mathcal{T}^{(0)} *_0^1 \mathcal{T}^{(1)} \times_0^2 \mathcal{T}^{(2)})$, which performs mode-(0, 0) partial outer product with $\mathcal{T}^{(0)}$, mode-(1, 0) convolution with $\mathcal{T}^{(1)}$ and mode-(2, 0) contraction with $\mathcal{T}^{(2)}$ simultaneously. In this case, a 5-order tensor $\mathcal{V} \in \mathbb{R}^{R \times X' \times P \times Q \times T}$ is returned, with entries calculated as

$$\mathcal{V}_{r, :, p, q, t} = \sum_{s=0}^{S-1} \mathcal{T}_{r,p}^{(0)} \left(\mathcal{U}_{r, :, s} * \mathcal{T}_{:,q}^{(1)} \right) \mathcal{T}_{s,t}^{(2)} \quad (14)$$

Identifying the best order to evaluate a compound operation with multiple tensors is in general an NP-hard problem, but for this example we can find it using exhaustive search:

$$\mathcal{V}_{r, :, p, q, t} = \left(\left(\sum_{s=0}^{S-1} \mathcal{U}_{r, :, s} \mathcal{T}_{s,t}^{(2)} \right) * \mathcal{T}_{:,q}^{(1)} \right) \mathcal{T}_{r,p}^{(0)} \quad (15)$$

If we follow the supplied brackets and break the evaluation into three steps, these steps take $O(RXST)$, $O(RXHPT)$ and $O(RX'HPT)$ operations respectively, therefore result in a total time complexity of $O(RXST + RXHPT + RX'PQT)$ for the compound operation.

Generally, compound operations over multiple tensors are difficult to flatten into mathematical equations, and usually described by *tensor diagrams* as in Section 2, which are usually called *tensor networks* [5] in the physics literature.

D Backpropagation of tensor operations

In order to use the operations in Appendix C in tensorial neural networks, we derive in this section their backpropagation rules. For brevity, we use tensor contraction as a tutorial example, and omit the derivations for other operations.

Tensor contraction Recall the definition of tensor contraction in Equations (8a) and (8b) in tensor algebra:

$$\mathcal{T} = \mathcal{T}^{(1)} \times \mathcal{T}^{(2)} \quad (16)$$

The partial derivatives of the result \mathcal{T} w.r.t. its operands $\mathcal{T}^{(0)}$, $\mathcal{T}^{(1)}$ can be computed at the entries level:

$$\frac{\partial \mathcal{T}_{i_0, \dots, i_{k-1}, i_{k+1}, \dots, i_{m-1}, j_0, \dots, j_{l-1}, j_{l+1}, \dots, j_{n-1}}}{\partial \mathcal{T}_{i_0, \dots, i_{k-1}, r, i_{k+1}, \dots, i_{m-1}}^{(0)}} = \mathcal{T}_{j_0, \dots, j_{l-1}, r, j_{l+1}, \dots, j_{n-1}}^{(1)} \quad (17a)$$

$$\frac{\partial \mathcal{T}_{i_0, \dots, i_{k-1}, i_{k+1}, \dots, i_{m-1}, j_0, \dots, j_{l-1}, j_{l+1}, \dots, j_{n-1}}}{\partial \mathcal{T}_{j_0, \dots, j_{l-1}, r, j_{l+1}, \dots, j_{n-1}}^{(1)}} = \mathcal{T}_{i_0, \dots, i_{k-1}, r, i_{k+1}, \dots, i_{m-1}}^{(0)} \quad (17b)$$

With chain rule, the derivatives of \mathcal{L} w.r.t. $\mathcal{T}^{(0)}$ and $\mathcal{T}^{(1)}$ can be obtained through $\partial \mathcal{L} / \partial \mathcal{T}$.

$$\frac{\partial \mathcal{L}}{\partial \mathcal{T}_{i_0, \dots, i_{k-1}, r, i_{k+1}, \dots, i_{m-1}}^{(0)}} = \sum_{j_0=0}^{J_0-1} \dots \sum_{j_{l-1}=0}^{J_{l-1}-1} \sum_{j_{l+1}=0}^{J_{l+1}-1} \dots \sum_{j_{n-1}=0}^{J_{n-1}-1} \frac{\partial \mathcal{L}}{\partial \mathcal{T}_{i_0, \dots, i_{k-1}, i_{k+1}, \dots, i_{m-1}, j_0, \dots, j_{l-1}, j_{l+1}, \dots, j_{n-1}}^{(1)}} \mathcal{T}_{j_0, \dots, j_{l-1}, r, j_{l+1}, \dots, j_{n-1}}^{(1)} \quad (18a)$$

$$\frac{\partial \mathcal{L}}{\partial \mathcal{T}_{j_0, \dots, j_{l-1}, r, j_{l+1}, \dots, j_{n-1}}^{(1)}} = \sum_{i_0=0}^{I_0-1} \dots \sum_{i_{k-1}=0}^{I_{k-1}-1} \sum_{i_{k+1}=0}^{I_{k+1}-1} \dots \sum_{i_{m-1}=0}^{I_{m-1}-1} \frac{\partial \mathcal{L}}{\partial \mathcal{T}_{i_0, \dots, i_{k-1}, i_{k+1}, \dots, i_{m-1}, j_0, \dots, j_{l-1}, j_{l+1}, \dots, j_{n-1}}^{(0)}} \mathcal{T}_{i_0, \dots, i_{k-1}, r, i_{k+1}, \dots, i_{m-1}}^{(0)} \quad (18b)$$

These tedious equations can be greatly simplified with tensor notations introduced before.

$$\frac{\partial \mathcal{L}}{\partial \mathcal{T}^{(0)}} = \text{swapaxes} \left(\frac{\partial \mathcal{L}}{\partial \mathcal{T}} \left(\times_0^{m-1} \circ \dots \circ \times_{l-1}^{m+l-2} \circ \times_{l+1}^{m+l-1} \circ \dots \circ \times_{n-1}^{m+n-3} \right) \mathcal{T}^{(1)} \right) \quad (19a)$$

$$\frac{\partial \mathcal{L}}{\partial \mathcal{T}^{(1)}} = \text{swapaxes} \left(\frac{\partial \mathcal{L}}{\partial \mathcal{T}} \left(\times_0^0 \circ \dots \circ \times_{k-1}^{k-1} \circ \times_{k+1}^k \circ \dots \circ \times_{m-1}^{m-2} \right) \mathcal{T}^{(0)} \right) \quad (19b)$$

where $\text{swapaxes}(\cdot)$ aligns the modes of outputs. Notice that the backpropagation equations are compound operations, even if the original operation is a basic one. The number of operations required for both backpropagation equations are $O(\left(\prod_{u=0}^{m-1} I_u\right) \left(\prod_{v=0, v \neq l}^{n-1} J_v\right))$, which are exactly the same as in the forward computation in Equation 16.

Tensor multiplication Recall the definition of tensor multiplication in Equations (9a) and (9b) in tensor algebra:

$$\mathcal{V} = \mathcal{U} \times_k \mathbf{M} \quad (20)$$

Backpropagation equations:

$$\frac{\partial \mathcal{L}}{\partial \mathcal{V}} = \frac{\partial \mathcal{L}}{\partial \mathcal{U}} \times_k \mathbf{M}^\top \quad (21a)$$

$$\frac{\partial \mathcal{L}}{\partial \mathbf{M}} = \mathcal{U} (\times_0^0 \circ \dots \circ \times_{k-1}^{k-1} \circ \times_{k+1}^{k+1} \circ \dots \circ \times_{m-1}^{m-1}) \frac{\partial \mathcal{L}}{\partial \mathcal{V}} \quad (21b)$$

The time complexities for both equations are $O((\prod_{u=0}^{m-1} I_u)J)$, which is identical to the forward computation in Equation (20).

Tensor convolution Recall the definition of tensor convolution in Equation (10a) in tensor algebra:

$$\mathcal{T} = \mathcal{T}^{(1)} *_l^k \mathcal{T}^{(2)} \quad (22)$$

Backpropagation equations:

$$\begin{aligned} \frac{\partial \mathcal{L}}{\partial \mathcal{T}^{(0)}} &= \text{swapaxes} \left(\frac{\partial \mathcal{L}}{\partial \mathcal{T}} (\times_0^m \dots \times_{l-1}^{m+l-1} \circ *_l^k \circ \times_{l+1}^{m+l-2} \circ \dots \circ \times_{n-1}^{m+n-2}) \text{flipaxis}(\mathcal{T}^{(1)}, l) \right) \\ &= \text{swapaxes} \left(\frac{\partial \mathcal{L}}{\partial \mathcal{T}} (\times_0^m \dots \times_{l-1}^{m+l-1} \circ (*_l^k)^\top \circ \times_{l+1}^{m+l-2} \dots \times_{n-1}^{m+n-2}) \mathcal{T}^{(1)} \right) \end{aligned} \quad (23a)$$

$$\begin{aligned} \frac{\partial \mathcal{L}}{\partial \mathcal{T}^{(1)}} &= \text{swapaxes} \left(\frac{\partial \mathcal{L}}{\partial \mathcal{T}} (\times_0^0 \circ \dots \circ \times_{k-1}^{k-1} \circ *_k^k \circ \times_{k+1}^{k+1} \circ \dots \circ \times_{m-1}^{m-1}) \text{flipaxis}(\mathcal{T}^{(0)}, k) \right) \\ &= \text{swapaxes} \left(\frac{\partial \mathcal{L}}{\partial \mathcal{T}} (\times_0^0 \circ \dots \circ \times_{k-1}^{k-1} \circ (*_k^k)^\top \circ \times_{k+1}^{k+1} \circ \dots \circ \times_{m-1}^{m-1}) \mathcal{T}^{(0)} \right) \end{aligned} \quad (23b)$$

where $(*_l^k)^\top$ is the *adjoint operator* of $*_l^k$. Without FFT, the time complexities for the equations are $O((\prod_{u=0, u \neq k}^{m-1} I_u) (\prod_{v=0, v \neq l}^{n-1} J_v) I_k J_l)$ and $O((\prod_{u=0, u \neq k}^{m-1} I_u) (\prod_{v=0, v \neq l}^{n-1} J_v) I_k I_k)$ respectively.

Tensor outer product Recall the definition of tensor outer product in Equation (11) in tensor algebra:

$$\mathcal{T} = \mathcal{T}^{(0)} \otimes \mathcal{T}^{(1)} \quad (24)$$

Backpropagation equations:

$$\frac{\partial \mathcal{L}}{\partial \mathcal{T}^{(0)}} = \frac{\partial \mathcal{L}}{\partial \mathcal{T}} (\times_0^m \circ \dots \circ \times_{n-1}^{m+n-1}) \mathcal{T}^{(1)} \quad (25a)$$

$$\frac{\partial \mathcal{L}}{\partial \mathcal{T}^{(1)}} = \frac{\partial \mathcal{L}}{\partial \mathcal{T}} (\times_0^0 \circ \dots \circ \times_{m-1}^{m-1}) \mathcal{T}^{(0)} \quad (25b)$$

The number of operations required for both equations are $O((\prod_{u=0, u \neq k}^{m-1} I_u) (\prod_{v=0}^{n-1} J_v))$.

Tensor partial outer product Recall the definition of tensor partial outer product in Equation (26):

$$\mathcal{T} = \mathcal{T}^{(0)} \otimes_l^k \mathcal{T}^{(1)} \quad (26)$$

Backpropagation equations:

$$\frac{\partial \mathcal{L}}{\partial \mathcal{T}^{(0)}} = \text{swapaxes} \left(\frac{\partial \mathcal{L}}{\partial \mathcal{T}} (\times_0^m \circ \dots \circ \times_{l-1}^{m+l-1} \circ \otimes_l^k \circ \times_{l+1}^{m+l-2} \circ \dots \circ \times_{n-1}^{m+n-2}) \mathcal{T}^{(1)} \right) \quad (27a)$$

$$\frac{\partial \mathcal{L}}{\partial \mathcal{T}^{(1)}} = \text{swapaxes} \left(\frac{\partial \mathcal{L}}{\partial \mathcal{T}} (\times_0^0 \circ \dots \circ \times_{k-1}^{k-1} \circ \otimes_k^k \circ \times_{k+1}^{k+1} \circ \dots \circ \times_{m-1}^{m-1}) \mathcal{T}^{(0)} \right) \quad (27b)$$

It is not difficult to show the time complexity for both equations above are $O((\prod_{u=0}^{m-1} I_u) (\prod_{v=0, v \neq l}^{n-1} J_v))$.

E Tensor decompositions

Tensor decompositions are natural extensions of matrix factorizations for multi-dimensional arrays. In this section, we will review three commonly used tensor decompositions, namely *CANDECOMP/PARAFAC (CP) decomposition* [21], *Tucker (TK) decomposition* [21] and *Tensor-train (TT) decomposition* [28].

CP decomposition CP decomposition is a direct generalization of singular value decomposition (SVD) which decomposes a tensor into additions of rank-1 tensors (outer product of multiple vectors). Specifically, given an m -order tensor $\mathcal{T} \in \mathbb{R}^{I_0 \times I_1 \times \dots \times I_{m-1}}$, CP decomposition factorizes it into m factor matrices $\{\mathbf{M}^{(l)}\}_{l=0}^{m-1}$, where $\mathbf{M}^{(l)} \in \mathbb{R}^{R \times I_l}, \forall l \in [m]$, where R is called the *canonical rank* of the CP decomposition, which is allowed to be larger than the I_l 's.

$$\mathcal{T}_{i_0, \dots, i_{m-1}} \triangleq \sum_{r=0}^{R-1} \mathbf{M}_{r, i_0}^{(0)} \dots \mathbf{M}_{r, i_{m-1}}^{(m-1)} \quad (28a)$$

$$\mathcal{T} \triangleq \sum_{r=0}^{R-1} \mathbf{M}_{r, :}^{(0)} \otimes \dots \otimes \mathbf{M}_{r, :}^{(m-1)} = \mathbf{1} \times_0^0 \left(\mathbf{M}^{(0)} \otimes_0^0 \dots \otimes_0^0 \mathbf{M}^{(m-1)} \right) \quad (28b)$$

where $\mathbf{1} \in \mathbb{R}^R$ is an all-ones vector of length R . With CP decomposition, \mathcal{T} can be represented with only $(\sum_{l=0}^{m-1} I_l)R$ entries instead of $(\prod_{l=0}^{m-1} I_l)$ as in the original tensor.

Tucker decomposition Tucker decomposition provides more general factorization than CP decomposition. Given an m -order tensor $\mathcal{T} \in \mathbb{R}^{I_0 \times I_1 \times \dots \times I_{m-1}}$, Tucker decomposition factors it into m factor matrices $\{\mathbf{M}^{(l)}\}_{l=0}^{m-1}$, where $\mathbf{M}^{(l)} \in \mathbb{R}^{R_l \times I_l}, \forall l \in [m]$ and an additional m -order core tensor $\mathcal{C} \in \mathbb{R}^{R_0 \times R_1 \times \dots \times R_{m-1}}$, where the *Tucker ranks* R_l 's are required to be smaller or equal than the dimensions at their corresponding modes, i.e. $R_l \leq I_l, \forall l \in [m]$.

$$\mathcal{T}_{i_0, \dots, i_{m-1}} \triangleq \sum_{r_0=0}^{R_0-1} \dots \sum_{r_{m-1}=0}^{R_{m-1}-1} \mathcal{C}_{r_0, \dots, r_{m-1}} \mathbf{M}_{r_0, i_0}^{(0)} \dots \mathbf{M}_{r_{m-1}, i_{m-1}}^{(m-1)} \quad (29a)$$

$$\mathcal{T} \triangleq \mathcal{C} \left(\times_0 \mathbf{M}^{(0)} \times_1 \mathbf{M}^{(1)} \dots \times_{m-1} \mathbf{M}^{(m-1)} \right) \quad (29b)$$

Notice that when $R_0 = \dots = R_{m-1} = R$ and \mathcal{C} is a super-diagonal tensor with all super-diagonal entries to be ones (a.k.a. identity tensor), Tucker decomposition reduces to CP decomposition, and therefore CP decomposition is a special case of Tucker decomposition. With Tucker decomposition, a tensor is approximately by $(\prod_{l=0}^{m-1} R_l + \sum_{l=0}^{m-1} I_l R_l)$ entries.

Tensor-train decomposition Tensor-train decomposition factorizes a m -order tensor into m interconnected low-order tensors $\{\mathcal{T}^{(l)}\}_{l=0}^{m-1}$, where $\mathcal{T}^{(l)} \in \mathbb{R}^{R_l \times I_l \times R_{l+1}}, l = 1, \dots, m-2$ with $\mathcal{T}^{(0)} \in \mathbb{R}^{I_0 \times R_0}$, and $\mathcal{T}^{(m-1)} \in \mathbb{R}^{R_{m-1} \times I_{m-1}}$ such that

$$\mathcal{T}_{i_0, \dots, i_{m-1}} \triangleq \sum_{r_0=1}^{R_0-1} \dots \sum_{r_{m-2}=1}^{R_{m-2}-1} \mathcal{T}_{i_0, r_0}^{(0)} \mathcal{T}_{r_0, i_1, r_1}^{(1)} \dots \mathcal{T}_{r_{m-2}, i_{m-1}}^{(m-1)} \quad (30a)$$

$$\mathcal{T} \triangleq \mathcal{T}^{(0)} \times_0^{-1} \mathcal{T}^{(1)} \times_0^{-1} \dots \times_0^{-1} \mathcal{T}^{(m-1)} \quad (30b)$$

where the R_l 's are known as *Tensor-train ranks*, which controls the tradeoff between complexity and accuracy of the representation. With Tensor-train decomposition, a tensor is represented by $(R_0 I_0 + \sum_{l=1}^{m-2} R_l I_l R_{l+1} + R_{m-1} I_{m-1})$ entries.

General tensor decompositions In this paper, we use the term tensor decomposition in a more general way, i.e. we do not stick to the standard formats defined in the previous paragraphs. Indeed, we consider tensor decomposition as a reverse mapping of tensor operations: consider a general tensor operation f on m input tensors $\{\mathcal{T}^{(l)}\}_{l=0}^{m-1}$ such that $\hat{\mathcal{T}} = f(\mathcal{T}^{(0)}, \dots, \mathcal{T}^{(m-1)})$ (i.e. $\hat{\mathcal{T}}$ is linear in each operand $\mathcal{T}^{(l)}$), the corresponding general tensor decomposition aims to recover the input factors $\{\mathcal{T}^{(l)}\}_{l=0}^{m-1}$ from a given tensor \mathcal{T} such that $\mathcal{T} \approx \hat{\mathcal{T}} = f(\mathcal{T}^{(0)}, \dots, \mathcal{T}^{(m-1)})$. In Figure 10, we demonstrate a few examples of general tensor decomposition using tensor diagrams.

Decomp.	Notations	$O(\# \text{ of params.})$	$O(\# \text{ of backprop ops.})$
original	\mathcal{T}	I	0
CP	$\mathbf{1} \times_0^0 (\mathbf{M}^{(0)} \otimes_0^0 \dots \otimes_0^0 \mathbf{M}^{(m-1)})$	$m I^{\frac{1}{m}} R$	$m I R$
TK	$\mathcal{C} (\times_0 \mathbf{M}^{(0)} \dots \times_{m-1} \mathbf{M}^{(m-1)})$	$R^m + m I^{\frac{1}{m}} R$	$m^2 I R$
TT	$\mathcal{T}^{(0)} \times_0^{-1} \dots \times_0^{-1} \mathcal{T}^{(m-1)}$	$m I^{\frac{1}{m}} R^2$	$m I R^2$

Table 8: **Summary of tensor decompositions.** In this table, we summarize three types of tensor decompositions in tensor notations, and list their numbers of parameters and time complexities to backpropagate the gradient of a tensor $\mathcal{T} \in \mathbb{R}^{I_0 \times I_1 \times \dots \times I_{m-1}}$ to its m factors (and an additional core tensor \mathcal{C} for Tucker decomposition). For simplicity, we assume all dimensions I_l 's of \mathcal{T} are equal, and denote the size of \mathcal{T} as the product of all dimensions $I = \prod_{l=0}^{m-1} I_l$. Furthermore, we assume all ranks R_l 's (in Tucker and Tensor-train decompositions) share the same number R .

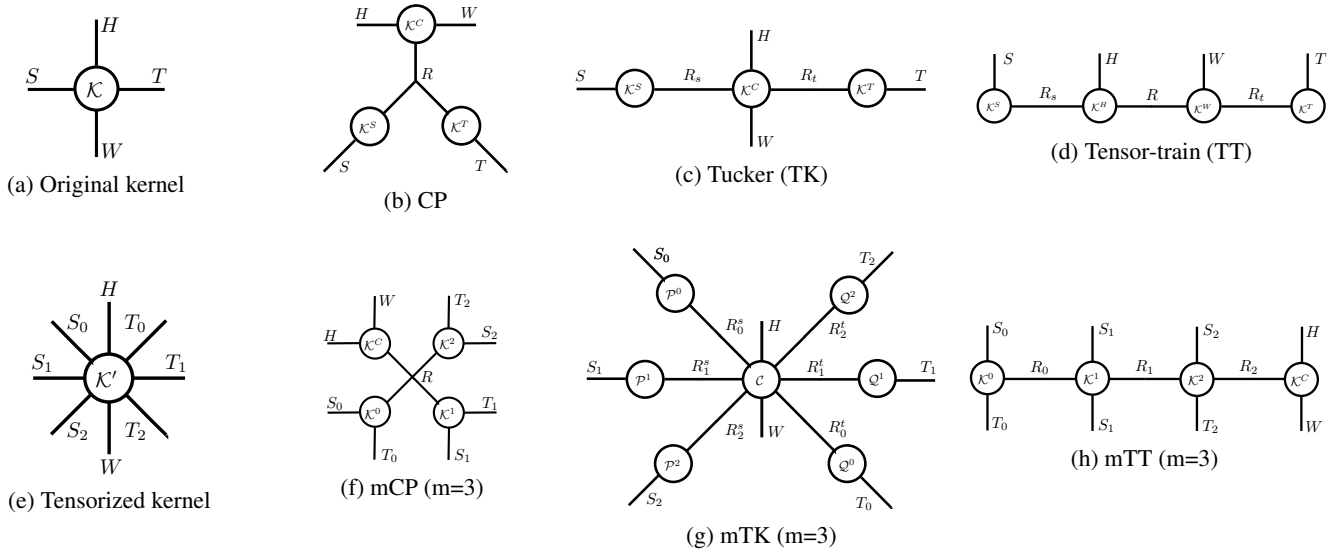


Figure 10: **Diagrams of general tensor decompositions.** Figures (a) and (e) are typical kernels of CNN and TNN respectively. Figures (b) (c) and (d) are three types of tensor decompositions on the convolutional kernel \mathcal{K} in (a). Figures (f) (g) and (h) are three types of general tensor decompositions for our tensorial kernel \mathcal{K}' in (e)

F Low-rank approximations of convolutional layer

In our paper, compact architecture of neural networks can be derived in two steps: (1) proposing an arbitrary architecture; and (2) decomposing the weights kernel at each layer into lower-order factors. When the proposed architecture is a standard convolutional neural network and the kernel is decomposed by traditional tensor decomposition, the derived architectures are known as low-rank approximations, in which each layer in the derived architecture is still a traditional operation (i.e. not general tensor operation).

Standard convolutional layer We review the standard convolutional neural network (CNN) for reference. In CNN, a convolutional layer is parameterized by a 4-order kernel $\mathcal{K} \in \mathbb{R}^{H \times W \times S \times T}$, where H and W are height and width of the filters (which are typically equal), S and T are the number of input and output channels respectively. A convolutional layer maps a 3-order tensor $\mathcal{U} \in \mathbb{R}^{X \times Y \times S}$ to another 3-order tensor $\mathcal{V} \in \mathbb{R}^{X' \times Y' \times T}$, where X and Y are the height and width for the input feature map, while X' and Y' are the ones for the output feature map, with the following equation:

$$\mathcal{V} = \mathcal{U} (*_0^0 \circ *_1^1 \circ \times_2^2) \mathcal{K} \quad (31)$$

Notice that the number of parameters in a standard convolutional layer is $HWST$ and the number of operations needed to evaluate the output \mathcal{V} is $O(HWSTXY)$.

SVD-convolutional layer In SVD-convolutional layer [18], the weights kernel \mathcal{K} is factorized by SVD.

$$\mathcal{K} = \text{swapaxes} \left(\mathcal{K}^{(0)} \times_1^2 \mathcal{K}^{(1)} \right) \quad (32)$$

where $\mathcal{K}^{(0)} \in \mathbb{R}^{H \times S \times R}$ and $\mathcal{K}^{(1)} \in \mathbb{R}^{W \times R \times T}$ are the two factor tensors. With two factors, the forward pass of SVD-convolutional layer is computed in two steps:

$$\mathcal{U}^{(0)} = \mathcal{U} (*_0^0 \circ \times_1^2) \mathcal{K}^{(0)} \quad (33a)$$

$$\mathcal{V} = \mathcal{U}^{(0)} (*_1^1 \circ \times_1^2) \mathcal{K}^{(1)} \quad (33b)$$

where $\mathcal{U}^{(0)}$ is an intermediate tensor after the first step. The backpropagation equations for these two steps are:

$$\frac{\partial \mathcal{L}}{\partial \mathcal{U}^{(0)}} = \frac{\partial \mathcal{L}}{\partial \mathcal{V}} \left((*_0^1)^\top \circ \times_2^2 \right) \mathcal{K}^{(1)}, \quad \frac{\partial \mathcal{L}}{\partial \mathcal{K}^{(1)}} = \mathcal{U}^{(0)} \left(\times_0^0 \circ (\overline{*_1^1})^\top \right) \frac{\partial \mathcal{L}}{\partial \mathcal{V}} \quad (34a)$$

$$\frac{\partial \mathcal{L}}{\partial \mathcal{U}} = \frac{\partial \mathcal{L}}{\partial \mathcal{U}^{(0)}} \left((*_0^0)^\top \circ \times_2^2 \right) \mathcal{K}^{(0)}, \quad \frac{\partial \mathcal{L}}{\partial \mathcal{K}^{(0)}} = \mathcal{U} \left((\overline{*_0^0})^\top \circ \times_1^1 \right) \frac{\partial \mathcal{L}}{\partial \mathcal{U}^{(0)}} \quad (34b)$$

CP-convolutional layer In CP-convolutional layer [9, 23], the weights kernel \mathcal{K} is factorized by CP decomposition.

$$\mathcal{K} = \mathbf{1} \times_2^0 \left(\mathcal{K}^{(1)} \otimes_1^2 \mathcal{K}^{(0)} \otimes_0^2 \mathcal{K}^{(2)} \right) \quad (35)$$

where $\mathcal{K}^{(0)} \in \mathbb{R}^{S \times R}$, $\mathcal{K}^{(1)} \in \mathbb{R}^{H \times W \times R}$ and $\mathcal{K}^{(2)} \in \mathbb{R}^{R \times T}$ are three factor tensors. With three factors, the forward pass of CP-convolutional consists of three steps:

$$\mathcal{U}^{(0)} = \mathcal{U} \times_2 \mathcal{K}^{(0)} \quad (36a)$$

$$\mathcal{U}^{(1)} = \mathcal{U}^{(0)} (*_0^0 \circ *_1^1 \circ \otimes_2^2) \mathcal{K}^{(1)} \quad (36b)$$

$$\mathcal{V} = \mathcal{U}^{(1)} \times_2 \mathcal{K}^{(2)} \quad (36c)$$

where $\mathcal{U}^{(0)} \in \mathbb{R}^{X \times Y \times R}$ and $\mathcal{U}^{(1)} \in \mathbb{R}^{X' \times Y' \times R}$ are two intermediate tensors, and the corresponding backpropagation equations can then be computed as:

$$\frac{\partial \mathcal{L}}{\partial \mathcal{U}^{(1)}} = \frac{\partial \mathcal{L}}{\partial \mathcal{V}} \times_2 (\mathcal{K}^{(2)})^\top, \quad \frac{\partial \mathcal{L}}{\partial \mathcal{K}^{(2)}} = \mathcal{U}^{(1)} (\times_0^0 \circ \times_1^1) \frac{\partial \mathcal{L}}{\partial \mathcal{V}} \quad (37a)$$

$$\frac{\partial \mathcal{L}}{\partial \mathcal{U}^{(0)}} = \frac{\partial \mathcal{L}}{\partial \mathcal{U}^{(1)}} ((*_0^0)^\top \circ (*_1^1)^\top \circ \otimes_2^2) \mathcal{K}^{(1)}, \quad \frac{\partial \mathcal{L}}{\partial \mathcal{K}^{(1)}} = \frac{\partial \mathcal{L}}{\partial \mathcal{U}^{(1)}} \left((\overline{*_0^0})^\top \circ (\overline{*_1^1})^\top \circ \otimes_2^2 \right) \mathcal{U}^{(1)} \quad (37b)$$

$$\frac{\partial \mathcal{L}}{\partial \mathcal{U}} = \frac{\partial \mathcal{L}}{\partial \mathcal{U}^{(0)}} \times_2 (\mathcal{K}^{(0)})^\top, \quad \frac{\partial \mathcal{L}}{\partial \mathcal{K}^{(0)}} = \mathcal{U} (\times_0^0 \circ \times_1^1) \frac{\partial \mathcal{L}}{\partial \mathcal{U}^{(0)}} \quad (37b)$$

TK-convolutional layer In TK-convolutional layer [19], the kernel \mathcal{K} is factorized by a partial Tucker decomposition,

$$\mathcal{K} = \mathcal{K}^{(1)} \left(\times_2 (\mathcal{K}^{(0)})^\top \times_3 \mathcal{K}^{(2)} \right) \quad (38)$$

where $\mathcal{K}^{(0)} \in \mathbb{R}^{S \times R_s}$, $\mathcal{K}^{(1)} \in \mathbb{R}^{H \times W \times R_s \times R_t}$ and $\mathcal{K}^{(2)} \in \mathbb{R}^{R_t \times T}$ are three factor tensors. Again, the forward pass of Tucker-convolutional layer has three steps:

$$\mathcal{U}^{(0)} = \mathcal{U} \times_2 \mathcal{K}^{(0)} \quad (39a)$$

$$\mathcal{U}^{(1)} = \mathcal{U}^{(0)} (*_0^0 \circ *_1^1 \circ \times_2^2) \mathcal{K}^{(1)} \quad (39b)$$

$$\mathcal{V} = \mathcal{U}^{(1)} \times_2 \mathcal{K}^{(2)} \quad (39c)$$

where $\mathcal{U}^{(0)} \in \mathbb{R}^{X \times Y \times R_s}$ and $\mathcal{U}^{(1)} \in \mathbb{R}^{X' \times Y' \times R_t}$ are two intermediate tensors. Their backpropagation equations are summarized as follows:

$$\frac{\partial \mathcal{L}}{\partial \mathcal{U}^{(1)}} = \frac{\partial \mathcal{L}}{\partial \mathcal{V}} \times_2 (\mathcal{K}^{(2)})^\top, \quad \frac{\partial \mathcal{L}}{\partial \mathcal{K}^{(2)}} = \mathcal{U}^{(1)} (\times_0^0 \circ \times_1^1) \frac{\partial \mathcal{L}}{\partial \mathcal{V}} \quad (40a)$$

$$\frac{\partial \mathcal{L}}{\partial \mathcal{U}^{(0)}} = \frac{\partial \mathcal{L}}{\partial \mathcal{U}^{(1)}} ((*_0^0)^\top \circ (*_1^1)^\top \circ \times_2^2) \mathcal{K}^{(1)}, \quad \frac{\partial \mathcal{L}}{\partial \mathcal{K}^{(1)}} = \frac{\partial \mathcal{L}}{\partial \mathcal{U}^{(1)}} \left((\overline{*_0^0})^\top \circ (\overline{*_1^1})^\top \right) \mathcal{U}^{(1)} \quad (40b)$$

$$\frac{\partial \mathcal{L}}{\partial \mathcal{U}} = \frac{\partial \mathcal{L}}{\partial \mathcal{U}^{(0)}} \times_2 (\mathcal{K}^{(0)})^\top, \quad \frac{\partial \mathcal{L}}{\partial \mathcal{K}^{(0)}} = \mathcal{U} (\times_0^0 \circ \times_1^1) \frac{\partial \mathcal{L}}{\partial \mathcal{U}^{(0)}} \quad (40c)$$

TT-convolutional layer TT-convolutional layer is derived by factorizing \mathcal{K} using Tensor-train decomposition.

$$\mathcal{K} = \text{swapaxes} \left(\mathcal{K}^{(0)} \times_0^{-1} \mathcal{K}^{(1)} \times_0^{-1} \mathcal{K}^{(2)} \times_0^{-1} \mathcal{K}^{(3)} \right) \quad (41)$$

where $\mathcal{K}^{(0)} \in \mathbb{R}^{S \times R_s}$, $\mathcal{K}^{(1)} \in \mathbb{R}^{R_s \times H \times R}$, $\mathcal{K}^{(2)} \in \mathbb{R}^{R \times W \times R_t}$ and $\mathcal{K}^{(3)} \in \mathbb{R}^{R_t \times T}$ are four factor tensors. The forward pass now contains four steps:

$$\mathcal{U}^{(0)} = \mathcal{U} \times_2 \mathcal{K}^{(0)} \quad (42a)$$

$$\mathcal{U}^{(1)} = \mathcal{U}^{(0)} (*_1^0 \circ \times_0^2) \mathcal{K}^{(1)} \quad (42b)$$

$$\mathcal{U}^{(2)} = \mathcal{U}^{(1)} (*_1^1 \circ \times_0^2) \mathcal{K}^{(2)} \quad (42c)$$

$$\mathcal{V} = \mathcal{U}^{(2)} \times_2 \mathcal{K}^{(3)} \quad (42d)$$

where $\mathcal{U}^{(0)} \in \mathbb{R}^{X \times Y \times R_s}$, $\mathcal{U}^{(1)} \in \mathbb{R}^{X' \times Y \times R}$ and $\mathcal{U}^{(2)} \in \mathbb{R}^{X' \times Y' \times R_t}$ are three intermediate results. Corresponding backpropagation equations for these computations are:

$$\frac{\partial \mathcal{L}}{\partial \mathcal{U}^{(2)}} = \frac{\partial \mathcal{L}}{\partial \mathcal{V}} \times_2 (\mathcal{K}^{(3)})^\top, \quad \frac{\partial \mathcal{L}}{\partial \mathcal{K}^{(3)}} = \mathcal{U}^{(2)} (\times_0^0 \circ \times_1^1) \frac{\partial \mathcal{L}}{\partial \mathcal{V}} \quad (43a)$$

$$\frac{\partial \mathcal{L}}{\partial \mathcal{U}^{(1)}} = \frac{\partial \mathcal{L}}{\partial \mathcal{U}^{(2)}} ((\times_0^1)^\top \circ \times_2^2) \mathcal{K}^{(2)}, \quad \frac{\partial \mathcal{L}}{\partial \mathcal{K}^{(2)}} = \mathcal{U}^{(1)} (\times_0^0 \circ \overline{(\times_1^1)^\top}) \frac{\partial \mathcal{L}}{\partial \mathcal{U}^{(2)}} \quad (43b)$$

$$\frac{\partial \mathcal{L}}{\partial \mathcal{U}^{(0)}} = \frac{\partial \mathcal{L}}{\partial \mathcal{U}^{(1)}} ((\times_0^0)^\top \circ \times_2^2) \mathcal{K}^{(1)}, \quad \frac{\partial \mathcal{L}}{\partial \mathcal{K}^{(1)}} = \mathcal{U}^{(0)} (\overline{(\times_0^0)^\top} \circ \times_1^1) \frac{\partial \mathcal{L}}{\partial \mathcal{U}^{(1)}} \quad (43c)$$

$$\frac{\partial \mathcal{L}}{\partial \mathcal{U}} = \frac{\partial \mathcal{L}}{\partial \mathcal{U}^{(0)}} \times_2 (\mathcal{K}^{(0)})^\top, \quad \frac{\partial \mathcal{L}}{\partial \mathcal{K}^{(0)}} = \mathcal{U} (\times_0^0 \circ \times_1^1) \frac{\partial \mathcal{L}}{\partial \mathcal{U}^{(0)}} \quad (43d)$$

Architect.	$O(\# \text{ of params.})$ $O(\# \text{ of forward ops.})$	$O(\# \text{ of backward ops. for inputs})$ $O(\# \text{ of backward ops. for params.})$
original	$HWST$ $HWSTXY$	$HWSTX'Y'$ $XYSTX'Y'$
SVD	$(HS + WT)R$ $HSXY + WTX'Y'R$	$(HSX'Y + WTX'Y')R$ $(XSX'Y + YTX'Y')R$
NN-CP	$(HW + S + T)R$ $(SXY + HWXY + TX'Y')R$	$(SXY + HWX'Y' + TX'Y')R$ $(SXY + XYX'Y' + TX'Y')R$
NN-TK	$(HWR_sR_t + SR_s + R_tT)$ $(HWR_sR_tXY + SR_sXY + R_tTX'Y')$	$(HWR_sR_tX'Y' + SR_sXY + R_tTX'Y')$ $(XYR_sR_tX'Y' + SR_sXY + R_tTX'Y')$
NN-TT	$(SR_s + HR_sR + WR_tR + R_tT)$ $(SR_sXY + HR_sRXY + WR_tRX'Y + R_tTX'Y')$	$(SR_sXY + HR_sRX'Y + WR_tTX'Y' + R_tTX'Y')$ $(SR_sXY + XR_sRXY + YR_tRX'Y' + R_tTX'Y')$

Table 9: **Summary of low-rank approximations of convolutional layer.** We list the number of parameters and the number of operations required by forward/backward passes for various low-rank approximations that compress convolutional layer. For reference, a standard convolutional layer maps a set of S feature maps with height X and width Y , to another set of T feature maps with height X' and width Y' . All filters in the convolutional layer share the same height H and width W .

G TNN based compression on dense layer

When the same technique in Appendix F is applied to compress the dense layer (a.k.a fully connected layer), we encounter one difficulty: the kernel in dense layer is a matrix and can not be further factorized by any tensor decomposition. In order to address this difficult, we define an equivalent *tensorized dense layer* that maps an m -order input tensor $\mathcal{U} \in \mathbb{R}^{S_0 \times \dots \times S_{m-1}}$ to another m -order tensor $\mathcal{V} \in \mathbb{R}^{T_0 \times \dots \times T_{m-1}}$ with a $2m$ -order kernel $\mathcal{K} \in \mathbb{R}^{S_0 \times \dots \times S_{m-1} \times T_0 \times \dots \times T_{m-1}}$.

$$\mathcal{V} = \mathcal{U} (\times_0^0 \circ \dots \circ \times_{m-1}^{m-1}) \mathcal{K} \quad (44)$$

The layer is equivalent to a standard dense layer if input \mathcal{U} , kernel \mathcal{K} and output \mathcal{V} are reshaped versions of their counterparts. Now we are ready to derive compact architectures for compression using general tensor decompositions.

mCP-dense layer The layer is derived if the kernel \mathcal{K} is factorized by a modified CP decomposition.

$$\mathcal{K} = \text{swapaxes} \left(\mathbf{1} \times_0^0 (\mathcal{K}^{(0)} \otimes_0^0 \dots \otimes_0^0 \mathcal{K}^{(m-1)}) \right) \quad (45)$$

where $\mathcal{K}^{(l)} \in \mathbb{R}^{R \times S_l \times T_l}$, $\forall l \in [m]$ are m factors. It results in a multi-steps procedure for forward pass:

$$\mathcal{U}^{(0)} = \mathbf{1} \otimes \mathcal{U} \quad (46a)$$

$$\mathcal{U}^{(l+1)} = \mathcal{U}^{(l)} (\otimes_0^0 \circ \times_1^1) \mathcal{K}^{(l)} \quad (46b)$$

$$\mathcal{V} = \mathbf{1} \times_0^0 \mathcal{U}^{(m)} \quad (46c)$$

where the m intermediate results $\mathcal{U}^{(l)} \in \mathbb{R}^{R \times S_l \times \dots \times S_{m-1} \times T_0 \times \dots \times T_{l-1}}, \forall l \in [m]$ are all $(m+1)$ -order tensors. Correspondingly, their backpropagation equations are computed as

$$\frac{\partial \mathcal{L}}{\partial \mathcal{U}^{(l)}} = \mathcal{K}^{(l)} \left(\otimes_0^0 \circ \times_{-1}^2 \right) \frac{\partial \mathcal{L}}{\partial \mathcal{U}^{(l+1)}} \quad (47a)$$

$$\frac{\partial \mathcal{L}}{\partial \mathcal{K}^{(l)}} = \mathcal{U}^{(l)} \left(\otimes_0^0 \circ \times_1^2 \circ \dots \circ \times_{m-1}^m \right) \frac{\partial \mathcal{L}}{\partial \mathcal{U}^{(l+1)}} \quad (47b)$$

$$\frac{\partial \mathcal{L}}{\partial \mathcal{U}^{(m)}} = \mathbf{1} \otimes \frac{\partial \mathcal{L}}{\partial \mathcal{V}}, \quad \frac{\partial \mathcal{L}}{\partial \mathcal{U}} = \mathbf{1} \times_0^0 \frac{\partial \mathcal{L}}{\partial \mathcal{U}^{(0)}}$$

mTK-dense layer The layer is obtained when a modified Tucker decomposition is used.

$$\mathcal{K} = \mathcal{C} \left(\times_0 (\mathbf{P}^{(0)})^\top \dots \times_{m-1} (\mathbf{P}^{(m-1)})^\top \times_m \mathbf{Q}^{(0)} \dots \times_{2m-1} \mathbf{Q}^{(m-1)} \right) \quad (48)$$

where $\mathbf{P}^{(l)} \in \mathbb{R}^{S_l \times R_l^s}, \forall l \in [m]$ are named as input factors, $\mathcal{C} \in \mathbb{R}^{R_0^s \times \dots \times R_{m-1}^s \times R_0^t \times \dots \times R_{m-1}^t}$ as core factor, and lastly $\mathbf{Q}^{(l)} \in \mathbb{R}^{R_l^t \times T_l}, \forall l \in [m]$ as output factors. The forward pass of mTK-dense layer can then be evaluated in three steps

$$\mathcal{U}^{(0)} = \mathcal{U} \left(\times_0 \mathbf{P}^{(0)} \dots \times_{m-1} \mathbf{P}^{(m-1)} \right) \quad (49a)$$

$$\mathcal{U}^{(1)} = \mathcal{U}^{(0)} \left(\times_0^0 \circ \dots \circ \times_{m-1}^m \right) \mathcal{C} \quad (49b)$$

$$\mathcal{V} = \mathcal{U}^{(1)} \left(\times_0 \mathbf{Q}^{(0)} \dots \times_{m-1} \mathbf{Q}^{(m-1)} \right) \quad (49c)$$

where $\mathcal{U}^{(0)}$ and $\mathcal{U}^{(1)}$ are two intermediate results. The backpropagation equations can then be derived accordingly:

$$\frac{\partial \mathcal{L}}{\partial \mathcal{U}^{(1)}} = \frac{\partial \mathcal{L}}{\partial \mathcal{V}} \left(\times_0 (\mathbf{Q}^{(0)})^\top \dots \times_{m-1} (\mathbf{Q}^{(m-1)})^\top \right) \quad (50a)$$

$$\left(\frac{\partial \mathcal{L}}{\partial \mathbf{Q}^{(l)}} \right)^\top = \frac{\partial \mathcal{L}}{\partial \mathcal{V}} \left(\times_0^0 \circ \dots \circ \times_{l-1}^{l-1} \circ \times_{l+1}^{l+1} \circ \dots \circ \times_{m-1}^{m-1} \right) \left(\mathcal{U}^{(1)} \left(\times_0 \mathbf{Q}^{(0)} \dots \times_{l-1} \mathbf{Q}^{(l-1)} \times_{l+1} \mathbf{Q}^{(l+1)} \dots \times_{m-1} \mathbf{Q}^{(m-1)} \right) \right) \quad (50b)$$

$$\frac{\partial \mathcal{L}}{\partial \mathcal{U}} = \frac{\partial \mathcal{L}}{\partial \mathcal{U}^{(0)}} \left(\times_0 (\mathbf{P}^{(0)})^\top \dots \times_{m-1} (\mathbf{P}^{(m-1)})^\top \right) \quad (50c)$$

$$\frac{\partial \mathcal{L}}{\partial \mathcal{U}^{(0)}} = \mathcal{C} \left(\times_0^m \circ \dots \circ \times_{m-1}^{2m-1} \right) \frac{\partial \mathcal{L}}{\partial \mathcal{U}^{(1)}} \quad (50d)$$

$$\frac{\partial \mathcal{L}}{\partial \mathcal{C}} = \mathcal{U}^{(0)} \otimes \frac{\partial \mathcal{L}}{\partial \mathcal{U}^{(1)}} \quad (50e)$$

$$\left(\frac{\partial \mathcal{L}}{\partial \mathbf{P}^{(l)}} \right)^\top = \frac{\partial \mathcal{L}}{\partial \mathcal{U}^{(0)}} \left(\times_0^0 \circ \dots \circ \times_{l-1}^{l-1} \circ \times_{l+1}^{l+1} \circ \dots \circ \times_{m-1}^{m-1} \right) \left(\mathcal{U} \left(\times_0 \mathbf{P}^{(0)} \dots \times_{l-1} \mathbf{P}^{(l-1)} \times_{l+1} \mathbf{P}^{(l+1)} \dots \times_{m-1} \mathbf{P}^{(m-1)} \right) \right) \quad (50f)$$

mTT-dense layer The layer [26] is derived by factorizing \mathcal{K} using a modified Tensor-train decomposition.

$$\mathcal{K} = \text{swapaxes} \left(\mathcal{K}^{(0)} \times_0^{-1} \mathcal{K}^{(1)} \times_0^{-1} \dots \times_0^{-1} \mathcal{K}^{(m-1)} \right) \quad (51)$$

where the factor tensors are $\mathcal{K}^{(l)} \in \mathbb{R}^{R_{l-1} \times S_l \times T_l \times R_l}, \forall l = 1, \dots, m-2$, with two corner cases $\mathcal{K}^{(0)} \in \mathbb{R}^{S_0 \times T_0 \times R_0}$ and $\mathcal{K}^{(m-1)} \in \mathbb{R}^{R_{m-2} \times S_{m-1} \times T_{m-1}}$.

$$\mathcal{U}^{(l+1)} = \mathcal{U}^{(l)} \left(\times_1^0 \circ \times_0^{-1} \right) \mathcal{K}^{(l)} \quad (52)$$

where $\mathcal{U}^{(0)} = \mathcal{U}, \mathcal{U}^{(m)} = \mathcal{V}$, and the other m tensors $\mathcal{U}^{(l)}$'s are intermediate results. Following Appendix D, its backpropagation equations can be derived as:

$$\frac{\partial \mathcal{L}}{\partial \mathcal{U}^{(l)}} = \mathcal{K}^{(l)} \left(\times_{-2}^1 \circ \times_{-1}^2 \right) \frac{\partial \mathcal{L}}{\partial \mathcal{U}^{(l+1)}} \quad (53a)$$

$$\frac{\partial \mathcal{L}}{\partial \mathcal{K}^{(l)}} = \text{swapaxes} \left(\mathcal{U}^{(l)} \left(\times_0^1 \circ \dots \circ \times_{m-2}^{m-1} \right) \frac{\partial \mathcal{L}}{\partial \mathcal{U}^{(l+1)}} \right) \quad (53b)$$

Architect.	$O(\# \text{ of params.})$	$O(\# \text{ of forward/backprop ops.})$
original	ST	ST
SVD	$(S+T)R$	$(S+T)R$
mCP	$m(ST)^{\frac{1}{m}}R$	$m \max(S, T)^{1+\frac{1}{m}}R$
mTK	$m(S^{\frac{1}{m}} + T^{\frac{1}{m}})R + R^{2m}$	$m(S+T)R + R^{2m}$
mTT	$m(ST)^{\frac{1}{m}}R^2$	$m \max(S, T)^{1+\frac{1}{m}}R^2$

Table 10: **Summary of TNN compression on dense layer.** In this table, we list the numbers of parameters and time complexities of forward/backward passes required by various TNN architectures that compress dense layer. For simplicity, we assume that the number of input units S and outputs units T are factorized evenly, i.e. $S_l = S^{\frac{1}{m}}, T_l = T^{\frac{1}{m}}, \forall l \in [m]$ and all ranks (in mTK and mTT) share the same number R , i.e. $R_l = R, \forall l \in [m]$.

H TNN compression on convolutional layer

Inspired by the reshaping trick in Appendix G, we develop three novel architectures that compress convolution layer by first proposing its higher-order counterpart: a *tensorized convolutional layer* maps $(m+2)$ -order tensor $\mathcal{U} \in \mathbb{R}^{X \times Y \times S_0 \times \dots \times S_{m-1}}$ to another $(m+2)$ -order tensor $\mathcal{V} \in \mathbb{R}^{X' \times Y' \times T_0 \times \dots \times T_{m-1}}$ with a $(2m+2)$ -order kernel $\mathcal{K} \in \mathbb{R}^{H \times W \times S_0 \times \dots \times S_{m-1} \times T_0 \times \dots \times T_{m-1}}$.

$$\mathcal{V} = \mathcal{U} \left(*_{0}^0 \circ *_{1}^1 \circ *_{2}^2 \circ \dots \circ *_{m+1}^{m+1} \right) \mathcal{K} \quad (54)$$

The tensorized convolutional layer is equivalent to standard convolutional layer if input \mathcal{U} , kernel \mathcal{K} and output \mathcal{V} are reshaped from their counterparts..

mCP-convolutional layer The layer is derived if the kernel \mathcal{K} is factorized by a modified CP decomposition as in Figure 10f.

$$\mathcal{K} = \text{swapaxes} \left(\mathbf{1} \times_0^0 \left(\mathcal{K}^{(0)} \otimes_0^0 \dots \otimes_0^0 \mathcal{K}^{(m)} \right) \right) \quad (55)$$

where $\mathcal{K}^{(l)} \in \mathbb{R}^{R \times S_l \times T_l}, \forall l \in [m]$ and $\mathcal{K}^{(m)} \in \mathbb{R}^{R \times H \times W}$ are $(m+1)$ factors. Accordingly, the multi-steps procedure to evaluate the output \mathcal{V} now has $(m+2)$ -steps:

$$\mathcal{U}^{(0)} = \mathbf{1} \otimes \mathcal{U} \quad (56a)$$

$$\mathcal{U}^{(l+1)} = \mathcal{U}^{(l)} \left(\otimes_0^0 \circ \times_1^3 \right) \mathcal{K}^{(l)} \quad (56b)$$

$$\mathcal{V} = \mathcal{U}^{(m)} \left(\times_0^0 \circ *_{1}^1 \circ *_{2}^2 \right) \mathcal{K}^{(m)} \quad (56c)$$

where $\mathcal{U}^{(l)} \in \mathbb{R}^{R \times S_l \times \dots \times S_{m+1} \times T_0 \times \dots \times T_{l-1}}, \forall l \in [m]$ are m intermediate tensors. The backpropagation equations of these steps above are

$$\frac{\partial \mathcal{L}}{\partial \mathcal{U}^{(m)}} = \mathcal{K}^{(m)} \left((*_0^1)^\top \circ (*_1^2)^\top \right) \frac{\partial \mathcal{L}}{\partial \mathcal{V}} \quad (57a)$$

$$\frac{\partial \mathcal{L}}{\partial \mathcal{K}^{(m)}} = \mathcal{U}^{(m)} \left((*_0^1)^\top \circ (*_1^2)^\top \times_2^3 \circ \dots \circ \times_{m+1}^{m+2} \right) \frac{\partial \mathcal{L}}{\partial \mathcal{V}} \quad (57b)$$

$$\frac{\partial \mathcal{L}}{\partial \mathcal{U}^{(l)}} = \text{swapaxes} \left(\mathcal{K}^{(l)} \left(\otimes_0^0 \circ \times_{-1}^2 \right) \frac{\partial \mathcal{L}}{\partial \mathcal{U}^{(l+1)}} \right) \quad (57c)$$

$$\frac{\partial \mathcal{L}}{\partial \mathcal{K}^{(l)}} = \mathcal{U}^{(l)} \left(\otimes_0^0 \circ \otimes_1^1 \circ \otimes_2^2 \circ \times_3^4 \circ \dots \circ \times_{m+2}^{m+3} \right) \frac{\partial \mathcal{L}}{\partial \mathcal{U}^{(l+1)}} \quad (57d)$$

$$\frac{\partial \mathcal{L}}{\partial \mathcal{U}} = \mathbf{1} \times_0^0 \frac{\partial \mathcal{L}}{\partial \mathcal{U}^{(0)}} \quad (57e)$$

mTK-convolutional layer The layer is derived if a modified TK decomposition as in Figure 10g on kernel \mathcal{K} .

$$\mathcal{K} = \mathcal{C} \left(\times_2 (\mathbf{P}^{(0)})^\top \dots \times_{m+1} (\mathbf{P}^{(m-1)})^\top \times_{m+2} \mathbf{Q}^{(0)} \dots \times_{2m+1} \mathbf{Q}^{(m-1)} \right) \quad (58)$$

where $\mathbf{P}^{(l)} \in \mathbb{R}^{S_l \times R_l^s}, \forall l \in [m]$, $\mathcal{C} \in \mathbb{R}^{H \times W \times R_0^s \times \dots \times R_{m-1}^s \times R_0^t \times \dots \times R_{m-1}^t}$ and $\mathbf{Q}^{(l)} \in \mathbb{R}^{R_l^t \times T_l}, \forall l \in [m]$ are named as input factors, core factor and output factors respectively. The forward pass of mTK-convolutional layer takes three steps:

$$\mathcal{U}^{(0)} = \mathcal{U} \left(\times_2 \mathbf{P}^{(0)} \dots \times_{m+1} \mathbf{P}^{(m-1)} \right) \quad (59a)$$

$$\mathcal{U}^{(1)} = \mathcal{U}^{(0)} \left(*_{0}^0 \circ *_{1}^1 \times_2^2 \circ \dots \circ \times_{m-1}^{m-1} \right) \mathcal{C} \quad (59b)$$

$$\mathcal{V} = \mathcal{U}^{(1)} \left(\times_2 \mathbf{Q}^{(0)} \dots \times_{m+1} \mathbf{Q}^{(m-1)} \right) \quad (59c)$$

where $\mathcal{U}^{(0)} \in \mathbb{R}^{X \times Y \times R_0^s \times \dots \times R_{m-1}^s}$ and $\mathcal{U}^{(1)} \in \mathbb{R}^{X' \times Y' \times R_0^t \times \dots \times R_{m-1}^t}$ are two intermediate tensors. The backpropagation equations can be derived similarly:

$$\frac{\partial \mathcal{L}}{\partial \mathcal{U}^{(0)}} = \mathcal{C} \left((*_0^0)^\top \circ (*_1^1)^\top \circ \times_2^{m+2} \circ \dots \circ \times_{m+1}^{2m+1} \right) \frac{\partial \mathcal{L}}{\partial \mathcal{U}^{(1)}} \quad (60a)$$

$$\frac{\partial \mathcal{L}}{\partial \mathcal{C}} = \mathcal{U}^{(0)} \left((*_0^0)^\top \circ (*_1^1)^\top \right) \frac{\partial \mathcal{L}}{\partial \mathcal{U}^{(1)}} \quad (60b)$$

mTT-convolutional layer The layer is derived by factoring \mathcal{K} according to a modified TT decomposition as in Figure 10h.

$$\mathcal{K} = \text{swapaxes} \left(\mathcal{K}^{(0)} \times_0^{-1} \mathcal{K}^{(1)} \times_0^{-1} \dots \times_0^{-1} \mathcal{K}^{(m)} \right) \quad (61)$$

where $\mathcal{K}^{(0)} \in \mathbb{R}^{S_0 \times T_0 \times R_0}$, $\mathcal{K}^{(l)} \in \mathbb{R}^{R_{l-1} \times S_l \times T_l \times R_l}$ and $\mathcal{K}^{(m)} \in \mathbb{R}^{R_{m-1} \times H \times W}$ are $(m+1)$ factor tensors. The multi-stages forward pass to evaluate \mathcal{V} now has $(m+1)$ steps:

$$\mathcal{U}^{(l)} = \mathcal{U}^{(l)} \left(\times_1^2 \circ \times_0^{-1} \right) \mathcal{K}^{(l)} \quad (62a)$$

$$\mathcal{V} = \mathcal{U}^{(m)} \left(*_1^0 \circ *_2^1 \circ \times_0^{-1} \right) \mathcal{K}^{(m)} \quad (62b)$$

where $\mathcal{U}^{(l)} \in \mathbb{R}^{X \times Y \times S_l \times \dots \times S_{m-1} \times T_0 \times \dots \times T_{l-1} \times R_{l-1}}$, $\forall l \in [m]$ are the intermediate results. We summarize the corresponding backpropagation equations as follows:

$$\frac{\partial \mathcal{L}}{\partial \mathcal{U}^{(m)}} = \frac{\partial \mathcal{L}}{\partial \mathcal{V}} \left((*_1^0)^\top \circ (*_2^1)^\top \right) \mathcal{K}^{(m)} \quad (63a)$$

$$\frac{\partial \mathcal{L}}{\partial \mathcal{K}^{(m)}} = \frac{\partial \mathcal{L}}{\partial \mathcal{V}} \left((*_0^0)^\top \circ (*_1^1)^\top \circ \times_2^2 \dots \times_{m+1}^{m+1} \right) \mathcal{U}^{(m)} \quad (63b)$$

$$\frac{\partial \mathcal{L}}{\partial \mathcal{U}^{(l)}} = \text{swapaxes} \left(\mathcal{K}^{(l)} \left(\times_{-2}^2 \circ \times_{-1}^3 \right) \frac{\partial \mathcal{L}}{\partial \mathcal{U}^{(l+1)}} \right) \quad (63c)$$

$$\frac{\partial \mathcal{L}}{\partial \mathcal{K}^{(l)}} = \text{swapaxes} \left(\mathcal{U}^{(l)} \left(\times_0^0 \circ \times_1^1 \circ \times_2^2 \dots \times_m^{m+1} \right) \frac{\partial \mathcal{L}}{\partial \mathcal{U}^{(l+1)}} \right) \quad (63d)$$

Architect.	O(# of params) O(# of forward ops.)	O(# of back ops. for inputs) O(# of back ops. for params.)
original	$HWST$ $HWSTXY$	$HWSTX'Y'$ $XYSTX'Y'$
TNN-mCP	$\#\text{Params}_{\text{CP}} + HW R$ $\#\text{Ops}_{\text{CP}} XY + HWTRXY$	$\#\text{Ops}_{\text{CP}} XY + HWTRX'Y'$ $\#\text{Ops}_{\text{CP}} XY + XYTRX'Y'$
TNN-mTK	$(HW \#\text{Params}_{\text{TK}_C} +$ $\#\text{Params}_{\text{TK}_I} + \#\text{Params}_{\text{TK}_O}$ $(HW \#\text{Ops}_{\text{TK}_C} XY +$ $\#\text{Ops}_{\text{TK}_I} XY + \#\text{Ops}_{\text{TK}_O} X'Y')$	$(HW \#\text{Ops}_{\text{TK}_C} X'Y' +$ $\#\text{Ops}_{\text{TK}_I} XY + \#\text{Ops}_{\text{TK}_O} X'Y')$ $(XY \#\text{Ops}_{\text{TK}_C} X'Y' +$ $\#\text{Ops}_{\text{TK}_I} XY + \#\text{Ops}_{\text{TK}_O} X'Y')$
TNN-mTT	$\#\text{Params}_{\text{TT}} + HW R$ $\#\text{Ops}_{\text{TT}} XY + HWTRXY$	$\#\text{Ops}_{\text{TT}} XY + HWTRX'Y'$ $\#\text{Ops}_{\text{TT}} XY + XYTRX'Y'$

[†]In order to compare against TNN based compressions on dense layer in Table 10, we denote the numbers for the dense layers as:

$$\begin{aligned} \#\text{Params}_{\text{CP}} &= m(S,T)^{\frac{1}{m}} R & \#\text{Params}_{\text{TK}} &= \sum_L \#\text{Params}_{\text{TK}_L} & \#\text{Params}_{\text{TT}} &= m(S,T)^{\frac{1}{m}} R^2 \\ \#\text{Ops}_{\text{CP}} &= m \max(S,T)^{1+\frac{1}{m}} & \#\text{Ops}_{\text{TK}} &= \sum_L \#\text{Ops}_{\text{TK}_L} & \#\text{Ops}_{\text{TT}} &= m \max(S,T)^{1+\frac{1}{m}} R^2 \\ \#\text{Params}_{\text{TK}_I} &= m S^{\frac{1}{m}} R & \#\text{Params}_{\text{TK}_C} &= R^{2m} & \#\text{Params}_{\text{TK}_O} &= m T^{\frac{1}{m}} R \\ \#\text{Ops}_{\text{TK}_I} &= m S R & \#\text{Ops}_{\text{TK}_C} &= R^{2m} & \#\text{Ops}_{\text{TK}_O} &= m T R \end{aligned}$$

Table 11: **Summary of TNN compression on convolutional layer.** In this table, we list the number of parameters and time complexities required by various TNN architectures that compress convolutional layer. Recall that a convolutional layer, composed with ST filters of size $H \times W$, maps a set of S feature maps of size $X \times Y$ to another set of T feature maps of size $X' \times Y'$. For simplicity, we assume the numbers of input/output feature maps S, T are factorized evenly, i.e. $S_l = S^{\frac{1}{m}}, T_l = T^{\frac{1}{m}}, \forall l \in [m]$, and all ranks are equal to R , i.e. $R_l = R, \forall l \in [m]$.